ERDC TR-11-1

US Army Corps
of Engineers®
Engineer Research and
Development Center

Tungsten Speciation in Firing Range Soils

Jay L. Clausen, Benjamin C. Bostick, Anthony Bednar,
Jing Sun and Joshua D. Landis

January 2011

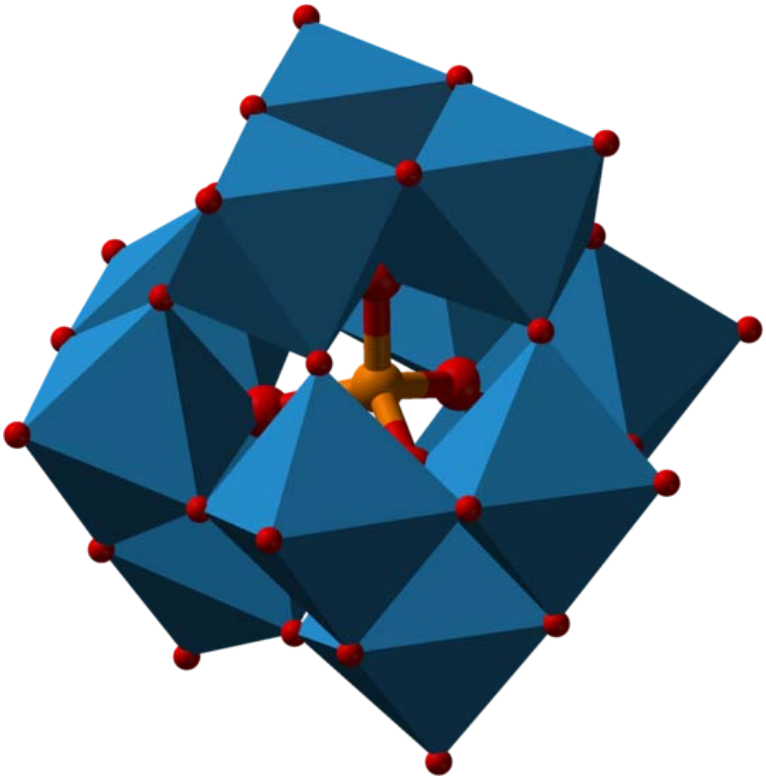

Engineer Research and
Development Center

COVER: Structure of a α-Keggin cluster with a Si/PW_{12} polymer consistent with the structure of tungsten in tungsten munitions-contaminated soils.

ERDC TR-11-1
January 2011

Tungsten Speciation in Firing Range Soils

Jay L. Clausen

Cold Regions Research and Engineering Laboratory
U.S. Army Engineer Research and Development Center
72 Lyme Road
Hanover, NH 03755

Benjamin C. Bostick

Columbia University
Lamont-Doherty Earth Observatory
Palisades NY 10964
and
Dartmouth College
Dept. of Earth Sciences
Hanover NH 03755

Anthony Bednar

Environmental Laboratory
U.S. Army Engineer Research and Development Center
3909 Halls Ferry Road
Vicksburg, MS 39180

Jing Sun, and Joshua D. Landis

Dartmouth College
Dept. of Earth Sciences
Hanover NH 03755

Final report

Prepared for U.S. Army Environmental Command
5179 Hoadley Road, Aberdeen Proving Ground, MD

Abstract: Synchrotron-based X-ray absorption spectroscopy (XAS) of select surface soil samples obtained from Camp Edwards, Massachusetts, small arms ranges indicate that little tungsten metal remains in the soil and that is not stable in the natural environment. X-ray absorption near edge structure (XANES) studies indicate rapid oxidation of tungsten metal to form tungsten oxides W(VI), polytungstates, tungstates, and polyoxometallates (POM) in any number of forms. Owing to structural similarities, it is difficult to identify specific species or discriminate between mineral species, although polytungstates and POMs predominate as compared to tungstates in soil. Additionally, this is the first study to identify the presence of tungsten POMs in soil.

XANES spectra indicated that, as depth increased, the fraction of soil sorbed tungstate increased and both polytungstate and POM decreased, suggesting POM and polytungstates are more stable in surface soils and likely to persist, whereas tungstate is unstable. Tetrahedral tungstate is unstable in neutral and acidic pH solutions such as are present in Camp Edwards surface soils, resulting in its conversion to a variety of polytungstates. Adsorption of tungstate, although weak, appears to occur on iron oxide surfaces such as ferrihydrite. XAS studies also revealed prevalence of adsorbed polytungstates rather than discrete mineral phases.

Soil pore waters in equilibrium with contaminated soils during laboratory experiments yielded tungsten concentrations in excess of 5000 mg L^{-1}, considerably in excess of predicted solubility limits of common tungsten minerals. These findings are consistent with field observations whereby tension lysimeters installed in the shallow vadose zone to monitor the soil pore water at the Bravo Range at Camp Edwards had tungsten concentrations as high as 400 mg L^{-1}. The high solubility and limited adsorption of tungsten in these soils is attributed to the formation of POMs such as $W_{12}SiO_{40}^{4-}$, an α-Keggin cluster, in soil solutions in addition to other polytungstates. Polytungstates are quite soluble and can yield water concentrations of several hundred mg L^{-1}. Although, not detected in groundwater, possibly because of analytical limitations, the presence of polytungstates in the vadose zone pore water at Camp Edwards suggests their presence cannot be completely ruled out. In contrast, the presence of tungstates in groundwater has been confirmed at Camp Edwards.

The weak retention of tungsten, in general to soils and observation of tungsten in soil pore water and groundwater at Camp Edwards attests to tungsten's potential mobility and transport in groundwater. The slow rates of conversion between POMs, polytungstates, and tungstates are likely to affect their solubility and transport considerably. Additionally, the presence of iron oxides such as ferrihydrite and organic matter may limit tungsten mobility. In general, tungsten mobility from highest to lowest proceeds from Tungstate→ Polytungstate → POM → Tungsten Oxide → Metallic Tungsten.

Table of Contents

List of Figures and Tables

Figures

Tables

Nomenclature

α–Keggin cluster Keggin structure is the best known structural form for heteropoly acids. It is the structural form of α–Keggin anions, which have a general formula of $[XM_{12}O_{40}]^{n-}$, where X is the heteroatom (most commonly P^{5+}, Si^{4+}, or B^{3+}), M is the addenda atom (most common are molybdenum and tungsten), and O represents oxygen. The structure self-assembles in acidic aqueous solutions and is the most stable structure of polyoxometallate catalysts

BET Brunauer-Emmett-Teller

CRREL Cold Regions Research and Engineering Laboratory

EDTA ethylenediamine tetraacetic acid

ERDC U.S. Army Engineer Research and Development Center

EXAFS extended X-ray absorption fine structure analysis

HPLC-ICP-MS High performance liquid chromatography-inductively coupled plasma-mass spectrometry

ICP-MS inductively-coupled plasma-mass spectroscopy

ICP-OES inductively-coupled plasma-optical emission spectroscopy

MMR Massachusetts Military Reservation

NSLS National Synchrotron Light Source

POM polyoxometallate

SEC-ICP-MS size-exclusion chromatography-inductively coupled plasma-mass spectrometry

SSRL Stanford Synchrotron Radiation Laboratory

TRIS tris(hydroxymethyl)methylamine

USAEC U. S. Army Environmental Command

W(VI) tungsten oxide

μXRF microprobe X-ray fluorescence

μXAS microprobe X-ray absorption

XANES X-ray absorption near edge structure

XAS	X-ray absorption spectroscopy
XRF	X-ray fluorescence

Preface

This report was prepared by Jay L. Clausen, Biogeochemical Sciences Branch (BSB), U.S. Army Engineer Research and Development Center (ERDC), Cold Regions Research and Engineering Laboratory (CRREL), Hanover, New Hampshire, Anthony Bednar ERDC-Environmental Laboratory (EL), Benjamin C. Bostick Columbia University, Jing Sun, and Joshua D. Landis, Dartmouth College, Dept. of Earth Sciences.

The U. S. Army Environmental Command (AEC) provided funding for this work. Dr. B. Packer (AEC) and Dr. S. Sobecki, CRREL, provided technical reviews.

The project team for this work includes the following:

- Technical Representative and Program Manager—Kimberly Watts (USAEC)
- Technical Project Manager—Dr. Bonnie Packer (USAEC)
- Principal Investigator—Jay Clausen (ERDC-CRREL)

Jay Clausen was responsible for communication with Kimberly Watts and Bonnie Packer of USAEC. The authors acknowledge the contributions of S. Taylor at CRREL

This report was prepared under the general supervision of Terrence Sobecki, Branch Chief, BSB, CRREL; Dr. Justin B. Berman, Research and Engineering Division Chief; Dr. Lance D. Hansen, Deputy Director, CRREL; and Dr. Robert E. Davis Director, CRREL. The Commander and Executive Director of the ERDC is Colonel Kevin Wilson. The Director is Dr. Jeffrey Holland.

Unit Conversion Factors

Multiply	By	To Obtain
cubic feet	0.02831685	cubic meters
cubic inches	1.6387064×10^{-5}	cubic meters
degrees Fahrenheit	(F-32)/1.8	degrees Celsius
feet	0.3048	meters
gallons (U.S. liquid)	3.785412×10^{-3}	cubic meters
inches	0.0254	meters
pounds (mass)	0.45359237	kilograms
pounds (mass) per cubic foot	16.01846	kilograms per cubic meter

1 Introduction

The U.S. Army Corps of Engineers, Engineer Research and Development Center, Cold Regions Research Engineering Laboratory (ERDC-CRREL), and Environmental Laboratory (ERDC-EL), were tasked by the U.S. Army Environmental Command (USAEC) to assess the fate-and-transport properties of tungsten leaching from tungsten-nylon bullets. The U.S. Army developed the tungsten-nylon bullet as a replacement for the lead bullet (Clausen et al. 2007). Metallic tungsten was believed to be essentially insoluble with little or no environmental mobility and thus environmentally benign. However, previous studies at Camp Edwards at the Massachusetts Military Reservation (MMR) demonstrate that powdered metallic tungsten used in these projectiles is mobile under some conditions (Clausen et al. 2007; Clausen and Korte 2009).

Prior to the previous decade, tungsten's environmental fate had not been studied in detail. Reasons included a lack of suitable analytical techniques as well as a general belief that tungsten was relatively insoluble and inert (Hartung 1991; Lassner et al. 1996; Langard 2001). This belief persisted even though the metallurgical literature had already suggested tungsten might be relatively soluble under appropriate conditions of pH and redox potential (Osseo-Asare 1982).

It is now known that, once deposited in metallic form, tungsten may be oxidized to soluble ions subject to leaching with percolating water. Therefore, the fate of tungsten ultimately depends on an accurate understanding of tungsten geochemistry. Unfortunately, the chemistry of tungsten in natural systems is not well understood; questions persist regarding what forms of tungsten are found in soils and to what extent solid-solution partitioning regulates tungsten concentrations.

The stable and soluble forms of tungsten under oxidizing conditions are tungstate (WO_4^{2-}) or oxide complexes in the +6 oxidation state. Study of tungsten's environmental behavior is complicated by its propensity to polymerize—a process favored at lower pH and higher tungsten concentrations—conditions potentially present in some firing range soils (Dermatas et al. 2004; Koutsospyros et al. 2006). Polymerization is the bonding of

two or more monomers, in this case tungstate, to form a polymer, i.e., polytungstate.

In principle, the thermodynamics of tungsten speciation are simple. Tungsten metal is unstable in the environment, and tungsten has for all practical purposes only one stable oxidation state, hexavalent tungstate (Baes and Mesmer 1986; Koutsospyros et al. 2006). Tungsten is nearly always found in one of a few mineral tungstates. In contrast to mineral forms, the solution chemistry of tungsten oxide complexes (Tungsten [VI]) is exceedingly complicated. Tungsten is similar to molybdate-forming variety of stable polyatomic anions, including $H_2W_{12}O_{40}^{-6}$, $HW_6O_{20}^{-3}$, and $W_6O_{20}(OH)^{-5}$ (Baes and Mesmer 1986). These species have well-known thermodynamic properties, with WO_4^{2-} stable in dilute and basic solutions, while the $W_{12}O_{40}^{-6}$ and related ions are stable in more concentrated solutions and acidic solutions. Within a narrow range of neutral pH, $W_6O_{20}(OH)^{-5}$ is also stable. Complications in tungsten speciation arise because interconversion among these forms is frequently slow, and numerous metastable ions, such as $W_4O_{12}(OH)_4^{-4}$, can persist in some solutions (Koutsospyros et al. 2006). However, the Koutsospyros et al. (2006) paper did not specify the rate of interconversion or degree of persistence.

Tungsten can also form a variety of polyoxometallates (POMs) in solution (Himeno et al. 2005; Chen et al. 2004). Polyoxometallates are cluster compounds containing two or more metal atoms that are similar in structure to polytungstates but are a different class of compound. Owing to structural similarities, it is difficult to distinguish between polytungstates and POMs. Tungsten POMs are constructed of WO_6 and a central MO_4 tetrahedron. One type of POM, known as an α-Keggin cluster ($MW_{12}O_{40}^{x-}$), has been intensively studied (Chen et al. 2004). Because of their exceptional size, molecular mass, structure, and chemical reactivity, a variety of other POMs are also known. Although some evidence suggests that such clusters are important in environmental systems (Furrer et al. 2002; Casey 2006), few studies have examined their formation in soils (Bednar et al. 2008). Furthermore, no thermodynamic data are available to predict the stability of tungsten POMs in soil systems, nor have they been conclusively identified in soils. Given the large molecular size of POMs, the expectation is that their mobility is low and thus would be retained in surface soil. Further, there is some evidence POMs are adsorbed onto soil to a greater extent than WO_4^{2-} and therefore are less mobile from a geochemical perspective.

Thermodynamic modeling of soil solutions with near-neutral pH based on known equilibria with common tungsten minerals (equilibrium with tungsten oxides including WO_3H_2O or $CaWO_4$) predicts tungstate concentrations of approximately 1 mg L^{-1}. In many cases, adsorption can keep tungsten concentrations much lower. Unfortunately, insufficient data are available to determine the reason for the high apparent solubility of tungsten in some soil environments and few studies have examined tungsten speciation in soils (Bednar et al. 2007, 2008). Certain questions have not been answered satisfactorily, such as: which tungsten mineral phase is present in soil and to what extent is adsorption important in regulating soil solution concentrations?

The operating conceptual model is that tungsten metal is deposited on the small arms firing range from the firing of a tungsten projectile. Upon impact with the soil surface, the tungsten-nylon pressed-powder core shatters, depositing micron-size tungsten metal particles. Tungsten metal rapidly oxidizes to form a tungsten oxide species W(VI) or WO_4^{2-}. The tungsten oxide is solublized and forms tungstates, polytungstates, and POMs species. Tungstate, under appropriate geochemical conditions, can also polymerize to form polytungstates. Depolymerization of polytungstate back to a tungstate is also a possibility, depending on the soil geochemistry.

During the oxidation process, a hydrogen ion (H^+) is released. If the tungsten mass is high enough and buffering capacity of the soil is low, acidification of the soil can occur, which could affect the speciation of tungsten, and the strength of tungsten adsorption. However, at Camp Edwards the surface soil is sufficiently acidic to favor polymerization of tungstate even without additional H^+ produced through oxidation. At some sites where the soil is borderline alkaline, polymerization would not occur on its own, but addition of H^+ from oxidation of metallic tungsten may be sufficient to start the polymerization processes. At sites where soil is sufficiently alkaline and the mass of tungsten introduced into the environment is low, polymerization of tungstate would not occur. If the rate of polymerization is slower than the precipitation infiltration rate, then tungstates will migrate deeper into the soil. If appropriate conditions are present at depth, tungstate will continue to polymerize to polytungstate as it moves downward. If the rate of polymerization is faster than the infiltration rate, polytungstate levels will build up in the shallow soil. Eventually, these polytungstates will be carried deeper into the soil profile. In contrast,

POM is strongly adsorbed to soil surfaces and, thus, is preferentially retained at the soil surface, unlike tungstate and polytungstate. So, in this report, we refer separately to tungstate, polytungstate, and POMs because of their different geochemical behavior and fate-and-transport properties. At Camp Edwards, then, the expectation is that the ratio of polytungstate to tungstate would increase with increasing depth and POM would remain tied up in the surface soil. A simplified conceptual model of tungsten mobility by soil depth is presented in Figure 1.

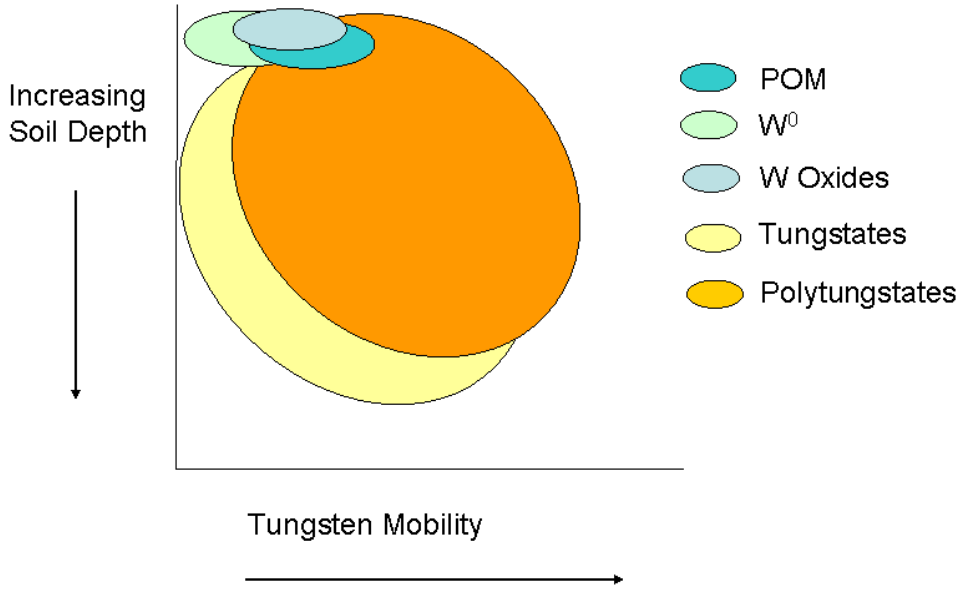

Figure 1. Conceptual relationship between tungsten mobility and soil depth.

Camp Edwards was chosen as a tungsten study site because tungsten-nylon projectiles had been fired there since October 1999 and detailed records were available for the number of bullets fired per range (Clausen et al. 2007). Tungsten measurements of soil and soil pore water at Camp Edwards found elevated levels present. Concentrations of tungsten in surface soils ranged as high as 2080 mg kg^{-1}. Samples from lysimeters installed into range berms showed tungsten in the soil pore water ranging to 400 mg L^{-1}. Samples from monitoring well MW-72S, located approximately 10 m down-gradient of the berm on Bravo Range, contained tungsten at levels between 0.005 and 0.560 mg L^{-1}. These findings raised concern that tungsten is migrating away from the small arms ranges and could affect down-gradient water supplies (Clausen et al. 2007).

This report is an extension of previous fieldwork documented in the Tungsten Phase I and Phase II Reports (Clausen et al. 2007, 2010) and fo-

cuses on tungsten speciation and solubility in a series of soils obtained from firing ranges where tungsten rounds were used. Aggregated, homogenized soil samples were collected from a variety of firing range sites at Camp Edwards (Clausen et al. 2007), and from two other sites: one in the northwestern U.S. and the other in the southeastern U.S (Clausen and Korte 2009). Mineral and adsorbed forms of tungsten were quantified using synchrotron-based X-ray absorption spectroscopy (XAS). Desorption isotherms for tungsten in these soils were used to characterize adsorbed phases. Results revealed complete and rapid oxidation of tungsten metal, and the prevalence of adsorbed polytungstates in soil solution rather than discrete mineral phases. Information provided in this report will assist the following organizations in future decision-making regarding tungsten's environmental behavior: U.S. Army, U.S. Army Environmental Command (USAEC), Impact Area Groundwater Study Program, and Massachusetts Army National Guard. It is expected that the U.S. Environmental Protection Agency, Massachusetts Department of Environmental Protection, and Environmental Management Commission for MMR should also find the information useful.

2 Objectives

The overall objective of this project was to develop an improved understanding of tungsten speciation in natural environments. This information is needed to accurately predict the fate of tungsten in firing range soils and in other contaminated environments. Thus, it is necessary to have a more complete understanding of tungsten geochemistry. Unfortunately, little is known about tungsten in environmental systems, and much of the data available concerning tungsten are conflicting. Field-based observations in some cases indicate that tungsten is highly soluble (Strigul et al. 2005; Bednar et al. 2008; Clausen and Korte 2009; Clausen et al. 2010), and tungstate adsorption to iron mineral phases in soil is strong, with rapid and complete adsorption under typical soil pH (Gustafsson 2003; Dermatas et al. 2004; Xu et al. 2006). To accurately assess the potential migration, and bioavailability, of tungsten (not the focus of this study), it is critical to understand tungsten's speciation or chemical form (focus of this study), and processes actively influencing its partitioning between soluble and insoluble mineral forms, and thus the extent to which these species are prone to leaching from surficial environments.

This research effort on tungsten-nylon fate and transport was divided into two phases. In the first phase, soil and soil pore water were sampled at three military installations; at one of the three installations, Camp Edwards, groundwater was also sampled (Clausen et al. 2007). Given that tungsten was detected in groundwater at Camp Edwards during four quarterly sampling efforts, a second phase of work (Clausen et al. 2010), focused on Camp Edwards, was funded to further understand the fate and transport of tungsten. In particular, the speciation work, which is the focus of this report, was funded in that second phase.

To meet the overall objectives for understanding tungsten migration and environmental behavior, the present study examined the speciation and solubility of tungsten in munitions-impacted soils primarily from three small arms firing ranges at Camp Edwards. A few samples from two other military installations were evaluated as points of comparison. X-ray absorption spectroscopy was used to determine the oxidation state of tungsten residues and to evaluate mineral and adsorbed forms of tungsten in these soils. This information is essential for evaluating the fate of

tungsten in these environments such that effective management decisions can be made regarding these training ranges. Investigations to identify tungsten-bearing phases included synchrotron-based microbeam spectroscopy, μ-X-ray fluorescence (μXRF) and μ-X-ray absorption (μXAS). Tungsten XAS has been applied to the study of tungsten catalysts and oxides (Michailovski et al. 2007; Montanari et al. 2008; Kelly et al. 2009), but has only recently been reported for natural materials (Bednar et al. 2008). Speciation data were then used to evaluate tungsten solubility from these soils using a series of desorption and sorption experiments. These data were used to propose a mechanistic link between tungsten speciation and solubility. Although these soils contain high levels of other metals (e.g., antimony, copper, lead, and zinc), the results gleaned from these studies should be generally applicable to an improved understanding of tungsten environmental geochemistry.

The tungsten work effort for Phase II was divided into a series of tasks. Task 1 consisted of development of a Work Plan for the field and laboratory studies. Tasks 2 through 5 included both field sampling of water and laboratory experiments. Tasks 6 and 7 involved groundwater modeling to predict migration rates through the unsaturated and saturated soil. Results from these tasks were reported elsewhere (Clausen et al. 2010). This report presents the findings of Task 8, a speciation study to ascertain the form or forms of tungsten present in the environment. Documentation of the results is Task 9. Detailed descriptions of each task are as follows, but note once again that only Task 8 is reported in this document.

- Task 1—Develop work plan.
- Task 2—Collect groundwater drive-point samples from several locations down gradient of the small arms ranges (Bravo and Southeast/Southwest Ranges) and install monitoring wells at (Bravo, Charlie, and Southeast/Southwest Ranges) at Camp Edwards to assess the nature and extent of tungsten and lead.
- Task 3—Install lysimeter clusters at depths of 1.5, 4.6, and 7.6 m (5, 15, and 25 ft) below ground surface at one location at the Bravo Range to assess the unsaturated zone transport rate of tungsten.
- Task 4—Determine tungsten dissolution rates from tungsten-nylon material via drip tests and conduct batch and column studies.
- Task 5—Do adsorption/desorption laboratory batch and column studies to quantify the interaction of tungsten and lead with MAECTITE™

treated surface soils, untreated surface soils, and subsurface soils under a variety of conditions.

- Task 6—Model the unsaturated zone to extrapolate from data collected in Tasks 2, 3, and 4 to predict tungsten transport rate across the entire unsaturated zone, i.e., approximately 36 m (120 ft),
- Task 7—Model groundwater using data from Tasks 2 through 6 to determine the tungsten transport rate and predicted extent in the saturated zone for all 12 small arms ranges at Camp Edwards.
- Task 8—Examine and explain the species of tungsten present in the environment.
- Task 9—Write Interim and Final Reports, documenting project management, and reporting.

3 Methods

High performance liquid chromatography-inductively coupled plasma-mass spectrometry (HPLC-ICP-MS) and size-exclusion chromatography-inductively coupled plasma-mass spectrometry (SEC-ICP-MS) were used to assess the species of tungsten present in water. Because tungsten can exist in multiple oxidation states and its speciation is poorly known, laboratory XAS, X-ray absorption near edge structure (XANES), extended X-ray absorption fine structure analysis (EXAFS), and X-ray microprobe analysis, including μXRF and μXAS, were used to identify and quantify the physical and chemical forms of tungsten in Camp Edwards soil cores and soil pore-water samples.

3.1 Site Selection and Sample Collection

Groundwater from monitoring wells, vadose zone pore water from tension lysimeters, and soil samples for speciation studies were collected as described previously (Clausen et al. 2007, 2010). Aggregated, homogenized soil samples were also collected from a variety of firing range sites at Camp Edwards (part of MMR), a northwestern U.S. site, and a southeastern U. S. site as previously described (Clausen et al. 2007; Clausen and Korte 2009). Tungsten munitions have been used at each of these ranges for as long as 5 years, and all were sampled within about 1 year (during 2006 and 2007) after tungsten usage ceased. Briefly, surface soil samples (0–5 cm depth) were collected from a variety of sites within the ranges, including firing points, the range floor, and at or beneath the targets and collection troughs. Additional sites at each location were selected as controls to examine background tungsten concentrations. Distribution of contaminants on ranges is variable because of the heterogeneous nature of their application. Therefore, each surface soil sample consisted of 100-increments following the *MULTI-INCREMENT*® sampling technique outlined in Hewitt et al. (2007). Soil samples were prepared following procedures outlined in Clausen et al. (2007, 2010). Briefly, the samples were sieved (to <2 mm) and homogenized (using a ball mill or mill grinder) prior to study. At two selected locations within the target zone, soil profiles were collected to 100 cm total depth to examine the tungsten vertical distribution. Identical depth intervals from four adjacent cores were aggregated to obtain representative soil samples, and each of these aggregated soil samples was sieved and homogenized prior to analysis.

3.2 Soil Analysis

3.2.1 Bulk Analysis

Soil samples for this effort had been collected and analyzed as part of Phase I activities (Clausen et al. 2007) prior to the current study. At that time, the bulk composition of soil samples was determined in the field using a field portable X-ray fluorescence (XRF) spectrometer (Innov-X Alpha-4000s) and in the laboratory by inductively coupled plasma-optical emission spectroscopy (ICP-OES) and ICP-mass spectrometry (ICP-MS). These earlier results are reported in Clausen et al. (2007, 2010).

Soil composition was determined a second time by Dartmouth College for this speciation work as part of Phase II activities by digesting 0.5-g aliquots of soil samples. As tungsten is relatively insoluble in acidic solutions, this digestion differs from most standard digestion procedures and those used by Clausen et al. (2007) during Phase I activities.

First, 0.5 g of homogenized soil was heated in 5 mL concentrated HNO_3 and 2 mL 30% H_2O_2 at 100°C, and this solution was evaporated to dryness. Once dry, 2 mL of concentrated HNO_3 was added to the digested soil and the solution again evaporated to dryness. Tungsten was recovered from the digested soil by dissolving the digestate in 2 mL of 20% NH_4OH, followed by sonicating and vortexing to ensure mixing. Once complete, 20 mL of a 2% NH_4OH/1% EDTA (ethylenediamine tetraacetic acid) solution was added and the resulting solution was filtered and diluted significantly (51 times, with a 0.2% NH_4OH/0.1% EDTA solution) prior to analysis using a Thermo Intrepid II inductively coupled plasma-optical emission spectrometer (ICP-OES). This instrument was operated in radial view, with blanks and quality control standards run every 5 samples, using drift-corrected standard curves. Use of NH_4OH and EDTA in the final extraction steps was necessary to maintain tungsten in soluble forms prior to analysis. Tungsten is spectrally rich, with several lines suitable for analysis. The 207.9-nm wavelength used for ICP-OES analysis had a detection limit of 6 $\mu g\ L^{-1}$, corresponding with a detection limit of <0.1 $mg\ kg^{-1}$ in the solid phase (accounting for any dilutions and digestion volumes).

3.2.2 X-Ray Absorption Spectroscopy

X-ray absorption spectroscopy was performed primarily on beam line 11-2 at the Stanford Synchrotron Radiation Laboratory (SSRL) located on Stan-

ford University in Menlo Park, California. Tungsten EXAFS analysis and XANES were also performed on a variety of samples. A 30-element germanium detector was used on beam line 11-2 (a 13-element detector was used on beam line 10-2 for some experiments) to collect absorption data in fluorescence mode. Sample slits for measurement configuration were 1 by 10 mm. The monochromator crystal reflection used was silicon (220) with a phi angle of 90°. Tungsten EXAFS spectra were collected from –235 to 900 eV about the tungsten L_3 edge. X-ray absorption near edge structure spectra were obtained at a sampling interval of 0.3 eV at the edge. Scans were calibrated by inflection of a tungsten metal foil to 10207.0 eV (the maximum in the first derivative).

All data averaging, normalization, and linear combination fitting was done with SIXPack software (Webb 2005). Spectra were then normalized with linear pre-edge and quadratic post-absorption edge functions. Resultant normalized XANES data were compared to a library of tungsten standards. The edge positions of the XANES spectra are mostly similar (the tungstates are all tetrahedral tungsten (VI), and thus all have similar edge shapes and spectral features). Normalized tungsten L_3-edge EXAFS spectra were converted to chi functions with k^3 weighting and then compared to reference spectra in an analogous process. Tungsten EXAFS and XANES spectra obtained for contaminated soils were also compared to a spectral library of commonly encountered reference compounds, including sodium tungstate (Na_2WO_4), sodium polytungstate ($Na_6[H_2W_{12}O_{40}]$), wolframite ($FeWO_4$), scheelite ($CaWO_4$), sodium phosphotungstate ($Na_4[PW_{12}O_{40}.nH_2O]$), tungsten oxide ($WO_3$), and tungsten metal ($W^0$) from commercial sources, as well as intact, fresh tungsten-nylon bullet cores. Mineral standards were obtained from the Dartmouth College Dana Mineral Collection, and chemical reference materials were obtained from Fisher Scientific or Strem Chemical (for the tungsten metal foil). All spectra were processed using SIXPack software (Webb 2005). Spectral processing included background subtraction, spectral normalization, and fitting a spline function to isolate scattering features. The resulting XANES and EXAFS spectra were then fit with linear combinations of similarly processed spectra obtained from pure reference materials. For final fitting, EXAFS spectra were fit to determine the relative concentration of each reference compound. Fitting yielded the fraction of each tungsten model compound within each sample. These fractions can then be converted to final soil concentrations by multiplying by the analyzed total solid concen-

trations from total digestion followed by ICP-OES (or XRF) analysis results.

Accuracy of least-squares fitting depends on the chosen reference standards representing the variation in the spectra of soil samples and having sufficiently different spectra that they can be differentiated. In this case, for example, tungsten metal from commercial sources (pure) could not be differentiated from the tungsten metal used in the bullet cores themselves, and only one metal standard is thus used in fitting. Similarly, true tungstates (not polytungstate or octahedral pseudotungstates) are all quite similar and difficult to differentiate in fitting. For this study, mineral reference spectra are chosen on the basis of known and inferred speciation and thermodynamics data, and mineral associations implied that are based on elemental correlations determined in X-ray microprobe analyses. Errors in least-squares fitting are best estimated based on comparisons of fits of known mixtures, which account for fitting error (usually small) and systematic errors such as in background fitting because of self absorption (particularly for XANES spectra)—which can be important when model compounds are used to represent complex mixtures. In the case of known mixtures, accuracy of fit depends on the quality of reference spectra (they should be noise "free," well calibrated, free of self absorption, etc.), the extent to which spectra are differentiated, and spectral processing. In the case of tungsten XANES, the sharp edges of tungsten compounds are separated by 2–3 eV (Kelly et al. 2009), which is large enough to calculate fractions of each oxidation state very accurately (to quantify the fraction of metallic tungsten for example); however, fitting of EXAFS spectra were used in all final fits to quantify each mineral component. In known mixtures, fractions of tungsten species are typically fit to within 3–4% of known ratios based on fits of spectra of mixtures containing equimolar mixtures of tungstate and tungsten metal. In general, the precision of results for EXAFS fitting is about 5% (O'Day et al. 2004), based on spectral fitting of mixtures with known composition.

3.2.3 X-ray Microprobe Measurements

Microprobe X-ray fluorescence (μXRF) was used to determine the distribution and association of tungsten with various mineral phases in soils. X-ray microprobe images were collected at the SSRL on beam line 2-3 or the National Synchrotron Light Source (NSLS) located at the Brookhaven National Laboratory in New York on beam line x26A. Both beam lines use Kirkpatrick-Baez focusing optics to focus the incident beam (to a nominal

beam size of 1–2 μm at SSRL, about 5 μm at NSLS). These samples were prepared by mounting a thin film of unconsolidated sediment grains on Kapton tape. X-Ray fluorescence spectra were collected at 13,000 eV by continuously rastering the beam across the sample every 5 μm (10 μm at NSLS), and measuring the XRF spectrum for 250 μs at each point (2 s at NSLS). Regions of interest were defined for a number of elements, including tungsten, calcium, copper, iron, manganese, potassium, silica, sulfur, titanium, and zinc, and the integrated counts for each were used to estimate elemental abundance. While counts are proportional to concentration, it is difficult to determine accurate concentrations from this method without standardization and accounting for variable sample thicknesses. Therefore, all data are presented as fluorescence counts, I_F, normalized to incident intensity I_0 (I_F/I_0). Because grain mounts are of variable thickness, sample absorbance ($\log(I_0/I_1)$) was used to estimate sample thickness and density—a plot of this absorbance (or transmittance, I_1/I_0) shows the distribution of grains quite clearly. The effect of variable thickness on elemental abundance can influence element correlations. This effect is accounted for by normalizing counts using transmittance; however, this normalization did not affect overall elemental correlations and is not used in the presented data.

One of the special qualities of X-ray microprobe measurements is that they allow both composition at high spatial resolutions (the grains scale), and they also have tunable (variable energy) X-ray sources that allow spectroscopy to be performed on specific locations within an X-ray map to conclusively identify individual grains. In particular, using the same instrument and optical configuration, it is possible to collect microprobe X-ray absorption spectra (μ-XAS) at specific regions on an individual grain of interest. This can be done using the microprobe beam lines at either beam line 2-3 at the SSRL or beam line X26a at the NSLS. For these μ-XAS measurements, regions of high and average tungsten concentration were chosen for XAS study, and XANES spectra were obtained (by varying the incident energy from below the L_3 edge of tungsten using a method similar to the method described above for bulk soils) at these points. In some cases, iron *K*-edge spectra also were obtained at the same point to correlate iron minerals to the presence of specific tungsten phases. Iron XANES spectra were obtained by varying the incident energy to the sample from about 100 eV below the iron *K*-edge (7112 eV) to about 200 eV above the edge. This method was highly successful at identifying specific minerals responsible for tungstate retention, and for identifying discrete tungsten miner-

als, which also have distinct iron spectra (if they contain iron). Linear-combination fitting was also used for these spectra, although in most cases only a single mineral phase is needed in fitting, in agreement with the observation that most measurements made are at the grain scale and thus are composed of single minerals. Iron minerals used in fitting included ferrihydrite, hematite, goethite, biotite, hornblende, and pyrite, which were obtained from the Dartmouth College Dana Mineral Collection. Linear combination fitting of iron spectra, however, is slightly less accurate for iron minerals (within about 7% for mixtures of Fe[III] oxides, better for reduced minerals) because many of the spectra are similar over a large *K*-range. Nevertheless, iron *K*-edge XANES is highly effective at identifying and quantifying crystalline iron oxides, ferrihydrite, iron silicates, and other phases in soils.

3.3 Desorption Isotherms

To better understand the nature of tungsten retention in soils, tungsten was equilibrated with soil water solutions to obtain desorption isotherms (Koopmans et al. 2004). A desorption isotherm for a single, representative contaminated soil (from a bullet pocket at Camp Edwards, sample MB036S3) was created by varying the solid-solution ratio between 0.2 and 6.8 g mL^{-1}(Appendix A). Subsamples of MB036S3 were made by adding different amounts of distilled water to a given dry mass of soil (between 30 and 120 mL were added to 12 to 300 g soil). Replicate samples were chosen for selected ratios to estimate sample homogeneity and found to yield results within 1% of dissolved tungsten. Resulting mixtures were equilibrated on a shaker table for 51 hours at 22°C. This length of time was chosen to allow the system to equilibrate, and was sufficient for tungsten concentrations in solution to stabilize. The resulting suspensions were centrifuged (4000 rpm for 10 minutes), and the solutions were filtered (with 0.2-µm Nylon filters) to remove residual solids. Unfiltered samples were also evaluated to determine the extent to which suspended colloids were present in the solution. These had identical concentrations to the filtered samples, indicating a lack of colloids, and are not discussed further. Filtered solutions were then divided into aliquots for tungsten analysis, major- and trace-element analysis, and pH measurements. Samples reserved for tungsten analysis were prepared by diluting 9:10 with a 2%NH_4OH/1%EDTA solution to preserve aqueous tungsten and analyzed immediately by ICP-OES as described in Section 3.2.1. Samples for major- and trace-elemental analysis were diluted 9:10 using 5% HNO_3 and determined immediately by ICP-OES using conventional methods. The pH was

not controlled in these measurements, but was buffered by reaction with soil minerals and was measured in final solutions using a standard, calibrated pH electrode. The total tungsten soil concentration of each sample was estimated on the basis of both soil digestions and XRF data; the residual concentration of solid-phase tungsten was determined using the total tungsten concentration and measured solution concentrations following equilibration.

Desorption experiments are useful to characterize the mechanisms of tungsten retention in soils. If a solid mineral phase limits concentrations, then the concentration of tungsten in solution should be constant and not depend on the level of tungsten in the solid phase, at least until the solid is no longer present, at which point the solution concentration will be controlled by the quantity of mineral in the system. In contrast, adsorption equilibria result in nonlinear relationships between solid- and aqueous-tungsten concentrations.

Tungsten in these systems is clearly controlled by adsorption processes, so resulting isotherm data are fit with both Langmuir and Freundlich isotherms. These isotherms are both commonly used to describe adsorption processes. The Langmuir isotherm is characteristic of a fixed number of sites of constant reactivity and usually is quite effective in describing adsorption of simple anions. The Langmuir isotherm has an adsorption maximum corresponding to the surface area of the solid. If solution concentrations are very high, then the surface will be fully saturated and any tungsten in the system will not be retained by the solid phase. In contrast, the Freundlich isotherm indicates a range in sites of differing energies and has no adsorption maximum. It is used to describe cation adsorption if cations can precipitate, but also can describe anion adsorption in some cases.

A single mean desorption isotherm for tungsten also was created using 23 representative soil samples (19 from Camp Edwards and 2 each from the southeastern and northwestern sites) at a constant solid–solution ratio. These soil samples were prepared as described above using a soil-to-solution ratio of 0.3 g mL^{-1}. The desorption test provides information on how strongly or weakly tungsten is adsorbed onto the soil surface and, combined with a speciation analysis, will show which species is preferentially desorbed.

3.4 Adsorption Isotherms

To better ascertain the role of adsorption on tungsten retention, a series of adsorption isotherms were calculated for tungstate adsorbing on ferrihydrite. Ferrihydrite was selected for these tests as earlier X-ray microprobe studies indicated that this was the primary iron species adsorbing tungstate. Ferrihydrite was synthesized using the method of Schwertmann and Cornell (1991) by rapidly titrating a $FeCl_3$ solution to pH 7 with sodium hydroxide. For these studies, W(VI) solutions (0–100 mg L^{-1}) were reacted with ferrihydrite suspensions (1 g L^{-1}) for 48 hours at room temperature. Tungsten was added as a sodium tungstate salt. Experiments were performed in 0.002 Molar tris(hydroxymethyl)methylamine (TRIS) buffer (adjusted to pH 7 with 0.1 M NaOH and HNO_3). Parallel isotherms were obtained for tungstate adsorption in the presence of 1 mg L^{-1} silicate (added from a stock solution of sodium silicate). Following equilibration, the pH was confirmed to be unchanged and the resulting suspension was sampled, filtered to remove solids, and preserved with a 2%NH_4OH/1%EDTA solution. The tungsten concentration of this solution was then determined immediately by ICP-OES as described previously to avoid the potential tungsten precipitation in mineral forms.

3.5 Solid-Solution Speciation Modeling

The geochemical model MINTEQ was used to predict the stable thermodynamic phases in desorption isotherm experiments, and the equilibrium tungstate adsorption in adsorption experiments. Visual MINTEQ v. 2.61 (Gustafsson 2009) is an equilibrium speciation model used to calculate the equilibrium composition of dilute aqueous solutions from adsorption–desorption experiments. MINTEQ is designed to describe aqueous speciation and mineral equilibria in soil environments, and has been recently updated to incorporate the latest thermodynamic data for all elements in solution. This is important for desorption experiments as many aqueous components are released into solution and an accurate assessment of their chemical forms is needed to properly describe tungsten solubility and complexation. In addition, this speciation program incorporates the most recent thermodynamic data for tungsten solids and solution complexes, and is particularly well suited for the study of ferrihydrite adsorption. Equations and equilibrium constants for tungstate, calcium, carbonate, and silica sorption to ferrihydrite were used without alteration, but include the most recent thermodynamic data for tungsten complexation and adsorption (Gustafsson 2003). It should be noted that no speciation

program contains formation constants for most complex tungstate ions, and only simple polytungstates are included because they are stable from a thermodynamic standpoint. However, numerous ion pairs and other polytungstates, including polyoxometallates containing tungsten and other elements, may exist in the solution for either thermodynamic or kinetic reasons, and these complexes may not be described using MINTEQ or other thermodynamic approaches. Equilibrium adsorption was modeled using a 2-pK diffuse layer model with a single surface site, with a specific surface area of ferrihydrite of 100 $m^2 g^{-1}$. The surface area of ferrihydrite in this system was determined using a 3-point (Brunauer-Emmett-Teller) BET isotherm with nitrogen gas. The model was modified for different experiments, to match their respective solid (ferrihydrite) to solution ratios, arsenic loadings, and solution compositions. MINTEQ's ferrihydrite adsorption database was used, which includes reactions and constants from Dzombak and Morel (1990), as well as updates with more recent thermodynamic data.

Adherence of observed adsorption data to theoretical models would suggest adsorption is well described in these soils with established chemical reactions, while significant deviations would indicate additional reactions not currently in the database need to be considered. This is likely because the MINTEQ databases, although the best available for tungsten complexes, still only contain a few of the myriad species that may be present in multi-component environmental solutions. Alternatively, and somewhat less likely, deviations may also indicate that the equilibria are correct but have improper equilibrium constants, possibly because they were derived from overly simplified experimental conditions.

3.6 Outdoor Dissolution Tests

Two tungsten/nylon cores were set outdoors in 2-cm-diameter Buchner funnels atop liter bottles. The two cores, labeled W1 (dark) and W2 (silver), weighed 2.06 and 2.07 g, respectively. Rainwater or snowmelt that fell onto the tungsten cores was collected in the bottles. Approximately every 2 weeks, the bottles were changed, the water volume measured and aliquots of the samples analyzed. No water samples were collected over the winter (December 2006–April 2007) when the experiment was covered with snow. The W1 core was sacrificed for other tests on November 2007 and the W2 test was stopped in July 2008. The details of this test are discussed in Clausen et al. (2010) and all data are provided in that document.

4 Results/Discussion

4.1 Tungsten in Soils

4.1.1 Soil Concentrations

Soil concentrations of tungsten varied widely within the firing range, and were generally much higher than background levels, about 1.5 mg kg^{-1} (Clausen and Korte 2009; Clausen et al. 2010). In impact berms, bullet pockets, and other areas directly receiving munitions, soil tungsten concentrations were as high as 5500 mg kg^{-1}. Concentrations varied widely and were generally much lower in other portions of the firing surface (Table 1, Clausen et al. 2010). Tungsten concentrations also dropped rapidly with soil depth. Composite soil depth profiles showed consistent trends in tungsten concentrations, with high concentrations in the surface soils, and dropping rapidly to near-background levels (1 to 2 mg kg^{-1}) at depth.

Although tungsten is concentrated at the soil surface, it is important to note that measurable tungsten is present at soil depths in excess of 50 cm. Tungsten munitions have been used for relatively short times at these ranges, less than 5 years. Detection at depths in excess of 50 cm implies tungsten has been transported downward from the soil surface where either intact tungsten bullets or bullet fragments were deposited. This transport may result from soil mixing but also suggests some fraction of the soil tungsten is labile and rapidly mobilized.

In summary, the following observations can be made about small arms range soils where tungsten-nylon projectile have been used:

- Soil tungsten concentration varied by site, with the highest concentrations observed at Camp Edwards, Massachusetts.
- At Camp Edwards, soil tungsten concentrations were a function of the number of tungsten projectiles fired.
- Tungsten soil concentration declined with increasing soil depth.

Table 1. Summary of tungsten concentrations for soil samples used in this study. Errors reported reflect the standard deviations of triplicate measurements where applicable.

Sample	Depth (cm)	pH	Organic Carbon (g kg^{-1})	Tungsten (mg kg^{-1})	Iron (g kg^{-1})	Calcium (g kg^{-1})
Camp Edwards Bravo Range						
"Profile A", in berm						
LB073B	0–25	6.1	12	887±60	3.3±0.4	28±4
LB074B	25–50	6.2	10	304±29	2.7±0.3	31±4
LB075B	50–75	6.3	9	122±22	2.9±0.3	23±5
LB076B	75–100	6.6	9	27±23	3.3±0.3	37±5
"Profile B", in trough						
Test 0005	0–5	6.2	10	5,081±132	11.0±0.5	20±8
Test 0510	5–10	6.3	9	4,204±900	10.0±0.6	19±6
Test 1015	10–15	6.4	8	1,223±76	6.2±0.6	21±7
Test 1520	15–20	6.5	10	516±53	4.3±0.7	19±3
Test 2025	20–25	6.6	11	466±38	10.2±0.4	19±11
Test 2530	25–30	6.6	11	353±71	4.3±0.3	20±4
Test 3040	30–40	6.8	11	393±74	4.8±0.5	25±6
Test 4050	40–50	6.7	12	342±34	5.4±0.4	24±5
Test 5060	50–60	6.8	10	160±26	3.6±0.8	19±4
Surface Samples						
MB022S1	0–5	6.4	9	2,356±402	5.0±0.6	21±6
MB023S2	0–5	6.3	11	1,548±171	4.9±0.5	21±9
MB030S1	0–5	6.5	8	3,248±1555	4.7±0.4	25±1
MB031S2	0–5	6.4	9	2,377±1124	4.7±0.7	22±6
MB032S3	0–5	6.8	12	2,709±513	4.1±0.7	25±4
MB036S3	0–5	6.7	12	1,626±450	3.8±0.6	23±6
Northwestern U.S. Site						
FL10	0–5	5.9	8	2,070±607	19±7	2.1±0.4
FL18	0–5	5.8	9	1,880±553	17±4	1.9±0.6
Southeastern U.S. Site						
B7	0–5	5.5	8	301±58	16±3	0.2
B9	0–5	5.4	9	112±30	19±3	0.3

4.1.2 Tungsten Speciation in Soil

4.1.2.1 X-Ray Absorption near Edge Structure Spectroscopy

X-ray absorption spectroscopy provides information about the oxidation state and speciation of tungsten in intact soils. This technique, therefore, can be useful for identifying and quantifying the presence of the various tungsten species and mineral forms present. For example, tungsten XANES was used to identify the fraction of metallic and oxidized tungsten in each soil sample. The XANES spectra of all soil samples overlapped and did not vary with depth or sampling location. The spectra of each soil sample contained an inflection edge at 10,210.9 eV followed by a strong white line feature at 10,213.5 eV (Fig. 2). These features are characteristic of tungstate, the fully oxidized W(VI) form stable in most soil environments. There were no observable spectral features at lower energy that is characteristic of metallic tungsten (which has an edge at 10,207.1 eV and considerably lower white line intensity), indicating little if any metallic tungsten was present in the soil samples.

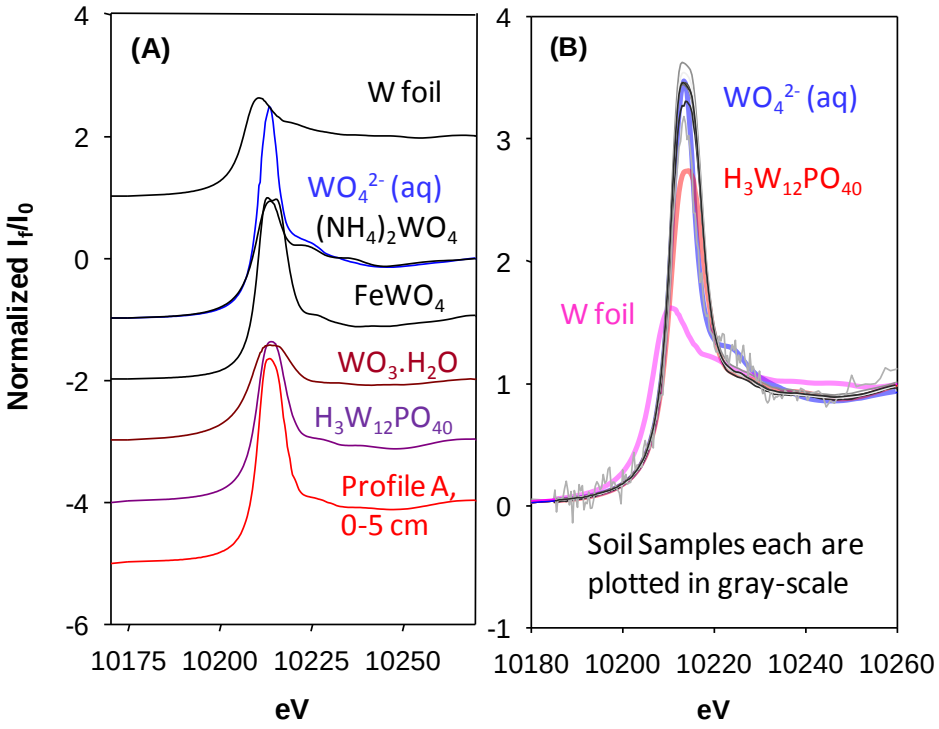

Figure 2. XANES spectra of selected reference materials (A) and (B) 10 representative soil samples from profiles A and B.

The position of oxidized W(VI) minerals is similar to all reference materials, and is easily distinguished from tungsten metal. The spectra of soils

are similar to that of tungstate (and polytungstate) and distinct from metallic tungsten. Least squares fitting of XANES spectra indicate >98% of the tungsten in each sample is W(VI). Further, these spectra indicate that tungsten metal in the munitions has been converted to tungstate, W(VI), or polytungstates of any number of forms, in the soil (Fig.3).

In summary, the XANES spectroscopy indicated the following:

- No tungsten metal is present in surface soils, indicating it is fully oxidized.
- Spectra indicate the presence of tungstate and polytungstate, suggesting the oxidized tungsten species are transitory and easily solublized.

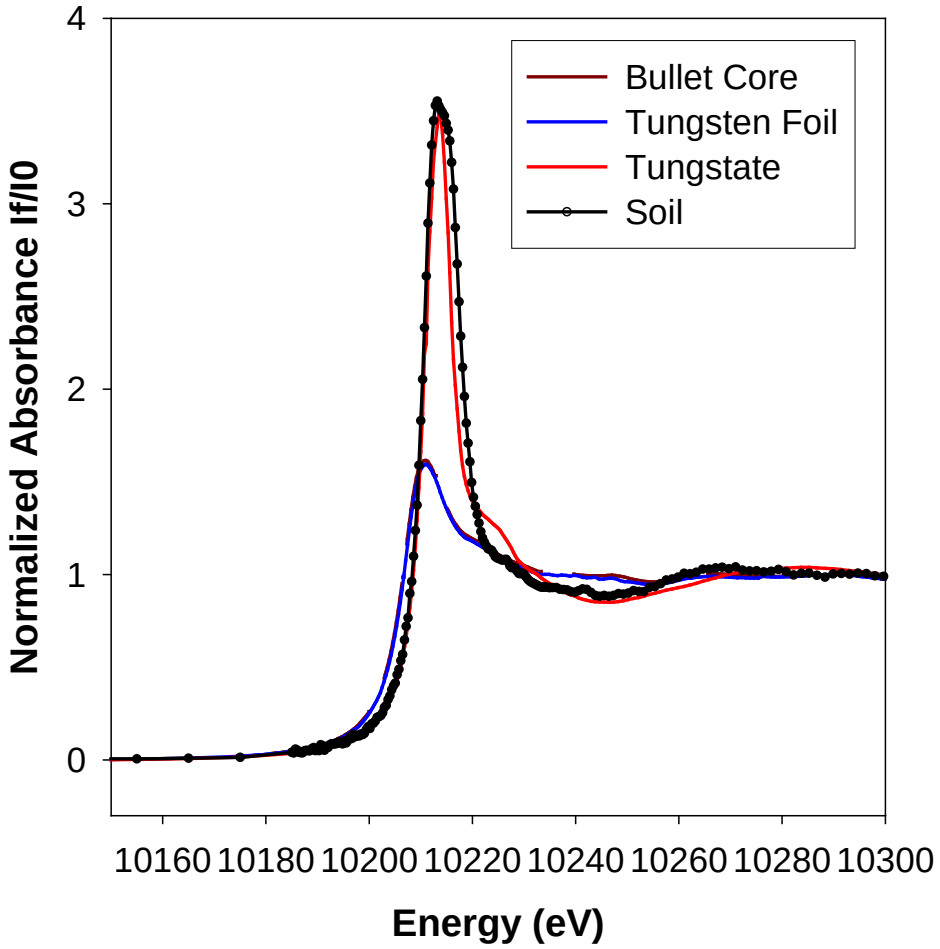

Figure 3. Tungsten L_3-edge XANES spectra of tungsten metal, tungsten in a bullet core compared to tungsten in soils, and tungstate (as sodium tungstate). Soils are nearly identical to tungstate. The spectrum of the bullet core is nearly the same as tungsten metal foil.

4.1.2.2 X-Ray Absorption near Edge Structure Interpretation

The fraction of tungsten metal and tungstate present in these samples was estimated using linear combination fitting of the XANES spectra. All spectra were adequately fit with only a single reference standard of sodium tungstate, with fits indicating 98% of tungsten in each sample was W(VI). This preponderance of oxidized tungsten has important implications for the fate of tungsten in the environment. Clearly, tungsten metal is not stable in soil environments. Tungsten was added to the soil as tungsten metal and had only a few years to oxidize. Given the limited time of environmental exposure, it is somewhat surprising the tungsten metal has rapidly and completely oxidized to tungstates and polytungstates. However, these results are consistent with the rapid release of dissolved tungsten from bullet cores as they react with water (Clausen et al. 2010). Furthermore, results indicate that the environmental fate of tungsten in these soils does not depend on the initial oxidation state of tungsten, as metallic tungsten (W^o) but rather depends on how oxidized tungstate species interact with soils.

The exact tungstate or polytungstate species sorbed to the soil is unknown, although precipitation of calcium and iron tungstates and polytungstates are possibilities (as will be discussed here), as are adsorption complexes on Fe(III) oxides (Gustafsson 2003). It is important to realize that the major form of tungsten in these samples is of critical importance for accurately assessing fate and transport. Occasionally, differences in the white line (the large peak in the XANES spectrum) intensity of tungstate and polytungstates can be used to differentiate between them (Pauporte et al. 2003). In our case, however, this distinction does not appear to be possible because the XANES spectra of different tungstates and polytungstates are sufficiently similar. The XANES spectra closely resemble polytungstate, and there is some evidence of splitting of the white line feature, which is also consistent with the spectra of polytungstates. The presence of polytungstates is more easily examined using EXAFS spectroscopy.

To summarize:

- Tungsten metal, W^o, from tungsten-nylon small arms ammunition is not stable in soil environments.
- Tungsten oxidation in the environment is not a limiting step in tungsten mobility.
- Mobilization of tungsten depends on how tungstate reacts with ions in the soil environment.

4.1.2.3 Extended X-ray Absorption Fine Structure Analysis Spectroscopy of Model Compounds

For extended EXAFS of tungsten to be used to characterize tungsten speciation in soils, it is necessary to collect spectra of prospective model compounds used as reference standards in fitting. Many of the spectra have not been published previously. These reference standards are used to establish that spectra are sufficiently different, and to confirm our methods are able to differentiate them.

Extended X-ray Absorption Fine Structure spectra depend on the structure of tungsten in a given mineral phase. For example, ammonium tungstate is a simple tungstate salt, with tungsten(VI) in tetrahedral coordination to four oxygen atoms. The EXAFS spectrum of tungstate is dominated by oscillations attributed to tungsten-oxygen (W-O) bonding (Fig. 4), and to few other features in the spectrum because the other atoms around tungsten are either light (low atomic number) or sufficiently far from the tungsten atom in the structure that they do not contribute to the spectrum.

Extended X-ray Absorption Fine Structure spectra can be used to determine the structure of atoms around a specific atom (in this case, tungsten). The ability to extract this structural information, and to do so without external standards, is quite powerful and is very useful to the study of structures for which we do not have model spectra. The structural data from known compounds can be compared with known structures for model compounds, but also yield new information used to characterize the mineral structure. Table 2 contains the structural data for the tungsten model compounds used in this study.

Tungsten model compounds can be separated into four principal groups: (1) tungsten metal; (2) true tungstates, WO_4^{2-}, which have tetrahedral tungstate; (3) complex metal tungstates containing disordered WO_6 polyhedra rather than tetrahedra; and (4) polytungstates and oxides, which also have disordered WO_6 polyhedra but also have tungsten-tungsten (W–W) shells. Each of these classes has distinct structural environments and is easily differentiated using EXAFS. Representative spectra from each of these classes of compounds are presented in Figure 4.

Tungsten metal has several W-W shells, which create a complex and well-defined interference pattern in the EXAFS spectrum that is easily differentiated from the other environments. This interference pattern results in

the presence of one or more nodes in the sine waves of the EXAFS spectrum (Fig. 4, left), where two waves deconstructively interfere, and spectral intensity (the *y*-axis) is diminished. Each wave creates one "peak" in the Fourier-transformed spectrum (Fig. 4, right). This Fourier transformed spectrum is called a radial structure function and can be imagined as a radial view of the density of atoms around the tungsten atom, with its size and shape depending on the element, its coordination number and its disorder; and its relative position determined by the distance of the atoms from the tungsten atom.

In contrast, tungstate spectra are much more complicated because the coordination environment of tungsten(VI) is highly variable. True tetrahedral tungstate (Class 2 in Table 2), although stable in alkaline solutions, converts to a variety of polytungstates in neutral and acidic pH solutions common to soils (Baes and Mesmer 1986; Koutsospyros et al. 2006). The spectrum of simple tungstate is dominated by a single, sharp W-O shell at 1.78 Å (Table 2). This shell is highly ordered, and is intense relative to other tungstates and polytungstates (Class 3 and 4 in Table 2), which have structures distinct from true tungstates.

The Class 3 and 4 tungstates and polytungstates are not true tungstates but instead are usually tungsten oxides, with complex W-O coordination because of multiple W-O shells. Many of these tungstates have tungsten in a disordered octahedral coordination to oxygen (coordination number 6). The highly disordered nature of the W-O shells makes the octahedral W-O shell have a much lower intensity than tetrahedral tungstates. The Class 4 polytungstates and tungsten oxides also usually contain a W-W shell because they are polymeric, and tungsten, if present in the local bonding environment, results in considerable scattering. The scattering results in a second peak in the Fourier-transformed spectra (Fig. 4, right side), making Class 4 polytungstates and tungsten oxides easy to differentiate from Class 3 tungstate minerals. In summary, each of the types of tungsten that could be encountered in the environment (Classes 1 to 4) have structural differences affecting their EXAFS spectra and provide a basis for identification and quantification in natural samples.

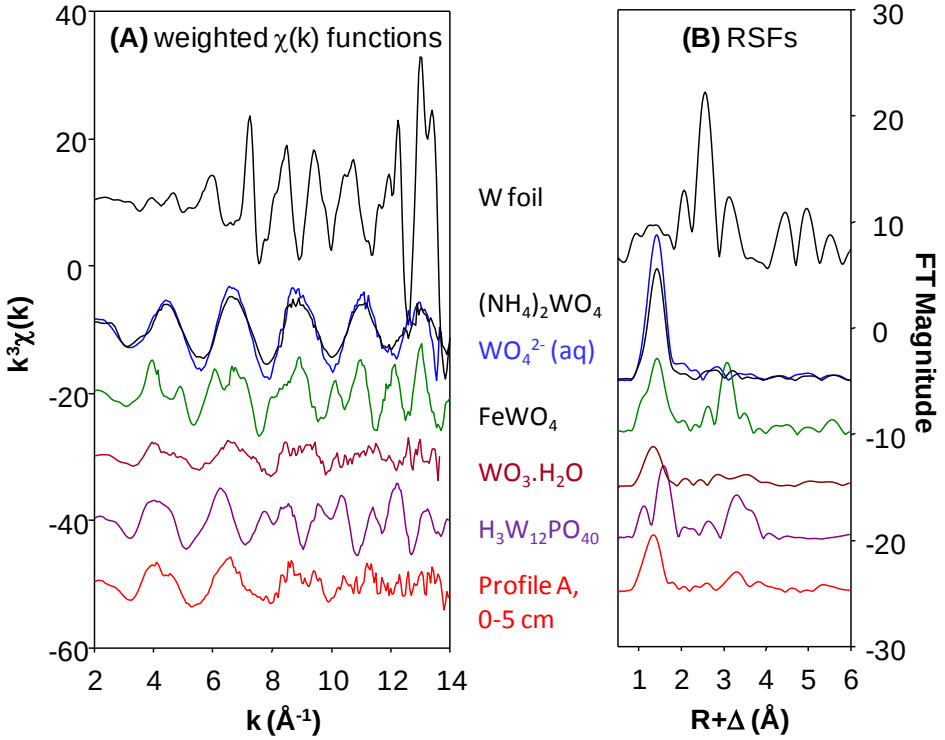

Figure 4. Chi functions (A) and radial structure functions (B) of select tungsten model compounds and a representative spectrum from soil profile A from the Camp Edwards site. Profile A consists of composite soil samples (MMRBLB073B, MMRBLB074B, and MMRLB075B) collected from the lower berm of Bravo Range at Camp Edwards near Targets 23, 26, 30, and 34.

In fact, tungstate minerals and polytungstates such as scheelite ($CaWO_4$) and wolframite ($FeWO_4$) are not true tungstates. Scheelite has disordered cubic coordination (Table 4), while wolframite is made up of WO_6 octahedra similar to those in polytungstates, and as a result, has similar spectra, with the exception that the second shells are of varying (smaller) intensities. Tungsten oxide, WO_3(s), is an insoluble oxide containing disordered WO_6 polyhedra linked in much the same fashion as polytungstates. The W-W distances in WO_3, however, are much longer than polytungstates (3.79 Å vs. 3.49–3.6 Å for $H_3W_{12}PO_{40}$), and the coordination numbers are higher, as would be expected of a condensed phase. Consequently, it should be possible to differentiate POMs and polytungstates from these W(VI) minerals based on their EXAFS spectra.

Table 2. EXAFS fitting parameters for select tungsten reference materials.

Sample	Shell	CN	R (Å)	σ^2 (Å^2)
Class 1: Tungsten Metal				
Tungsten metal (from bullet core)	W-W	8[a]	2.74	0.005
	W-W	6[a]	3.16	0.005
	W-W	12[a]	4.47	0.008
	W-W	24,8[a]	5.24,5.48	0.01
Class 2: True tungstates				
$(NH_4)_2WO_4$	W-O	4	1.78	0.003
WO_4^{2-} solution @ pH 10	W-O	4	1.78	0.003
Class 3: Metal Tungstates				
$CaWO_4$(s) (De Buysser et al. 2008)	W-O	4[a]	1.78	0.005
	W-O	4[a]	2.90	0.005
	W-Ca	4[a]	3.70	0.005
	W-W/Ca	4,4[a]	3.85	0.005
$FeWO_4$(s)	W-O	4[a]	1.94	0.004
	W-O	2[a]	2.11	0.004
	W-W	2,2[a]	3.23,4.42	0.006
	W-Fe	4,4[a]	3.53,3.74	0.006,0.011
Class 4: polytungstates and tungsten oxides				
W(VI) solution pH 6.7 (predicted species is $W_7O_{24}^{6-}$)	W-O	2[a]	1.78	0.005
	W-O	4[a]	1.93	0.008
	W-W	2.8	3.75	0.011
WO_3(s) (Martin et al. 1998)	W-O	2.8	1.79	0.003
	W-O	2.6	2.12	0.008
	W-W	5.6	3.79	0.010
	W-W	1.2	3.87	0.012
$W_{12}SiO_{40}^{4-}$ (Martin et al., 1998)	W-O	1.3	1.72	0.002
	W-O	4.2	1.92	0.006
	W-W	2.7	3.34	0.009
	W-W	2.1	3.71	0.010
$H_3W_{12}PO_{40}$ .nH_2O	W-O	1.7	1.70	0.002
	W-O	4[a]	1.88	0.006
	W-W	2[a]	3.49	0.003
	W-W	2[a]	3.63	0.011

(a): Fixed during fitting based on crystallographic data. The coordination number (CN) is typically accurate to within ±1, inter-atomic distance (R) within ± 0.02 angstroms (Å); σ^2 represents the variance in R (in Å^2). For all of the reference materials, E^0 was ≈ 10,211 eV, except tungsten metal, which was 10,207 eV.

One interesting class of tungstates that may be adsorbed in soils systems are the POMs, and it is important to understand their structure and spectra so that we might identify them if present in soil environments. Numerous POMs of tungsten exist (Chen et al. 2004) but little is known about their existence in environmental systems, although some data suggest such complexes could form in soils (Bednar et al. 2007, 2008). Although a number of POMs can form readily with common ions in solution (e.g., silicate, phosphorous), no thermodynamic data exist in the literature on the stability of such complexes in aqueous solutions, or for their adsorption to soil minerals. In other words, information useful for predicting POM prevalence in environmental systems is lacking and POMs have not been observed directly in soils prior to this study. Tungsten POMs are similar in structure to polytungstates, which makes it difficult to differentiate between POMs and other polytungstates based on EXAFS alone.

While the identity and distances to the heteroatoms (the metals other than tungsten in the structure of POMs) are in principle useful to differentiate between different POMs (Manceau 1995, Manning et al. 1998, Morin et al. 2008) and tungstates, identification is complicated for POMs. POMs and other polytungstates also contain W-W shells that are intense and mask the effect of a single, smaller atom such as Si and these W-W shells, making it difficult to conclusively identify which POM, if any, is present in soils.

The structure and EXAFS spectrum of two common and potentially relevant POMs is known. In the spectra of silicotungstate and phosphotungstate, two substituted POMs, there are two W-O shells, at about 1.7 and 1.9 Å, respectively, that are similar to the bonding environment of both class 3 and 4 tungstates in Table 2. The similarity with “simple polytungstates” and tungsten oxides (Class 4 compounds), however, make it much more complicated to identify specific polytungstate phases, or to differentiate polytungstates from mineral phases. In fact, polytungstates and many tungstate minerals are each composed of disordered WO_6 octahedra with similar bond distances, and each has second shells between 3 and 4.5 Å in the radial structure function attributable to tungsten-tungsten (W-W) or other shells. These second shells are quite complex and are composites of a number of different structural components of similar distance, and in many cases, destructive interference between these many structural components lowers the overall intensity of the second shell. This structural he-

terogeneity between these materials is sufficient to complicate spectral fitting even for pure reference compounds with known structures.

To summarize:

- EXAFAS can differentiate among mineral tungstates, adsorbed tungstate, and polytungstates based on their structural differences.
- Even with the use of EXAFS, it is exceedingly difficult to identify specific polytungstate species or discriminate between mineral phases.
- Additionally, POMS are similar in structure to polytungstates thus differentiation with EXAFS is difficult.

4.1.2.4 EXAFS Interpretation of Tungsten Speciation in Contaminated Soils

The accurate quantification of tungsten species in contaminated soil depends on fitting the EXAFS spectra of soils with linear combinations of known reference spectra. The effective implementation of linear combination fitting depends on the unique spectral signature of each model compound identified in the soils. In principle, the reference spectra for each model compound have unique characteristics, allowing each to be fit independently; however, the similarities in spectra required the aggregation of model compounds into representative components that were sufficiently distinct spectrally. Moreover, some polytungstates, such as $W_6O_{20}(OH)^{5-}$, may be found in soils, particularly at near-neutral pH (Baes and Mesmer 1986; Koutsospyros et al. 2006), but no reference spectra are available for such materials. To address these limitations, least squares fitting of EXAFS spectra was performed using only four reference spectra: tungsten metal, tungstate solution (representative of Class 2 true tungstates, adsorbed tungstate, and WO_4^{2-}), wolframite (a Class 3 tungstate: a model tungsten(VI) mineral solid), and $H_3PW_{12}O_{40}$ (a Class 4 polytungstate: a model POM with known structure and spectrum). Attempts at fitting with WO_3, H_2O, and $CaWO_4$ did not yield stable fits owing to their similarity with $FeWO_4$. These four reference spectra should be regarded as model compounds representative of tungsten mineral classes rather than discrete species because of spectral similarities. For example, fitting with $H_3PW_{12}O_{40}$ does not imply that phosphotungstic acid is present in soils (although it may well be considering that the soil was treated with MAECTITE™—a phosphate based fixation agent), rather it is representative of polytungstates more generally. The implication is that it is not impossible to more conclusively identify POMs, or specific mineral phases, but such determinations depend on W-W distances and coordination

numbers obtained from conventional fitting of selected spectra. Other analytical methods, including X-ray fluorescence, also can be used to establish mineral phases based on composition.

In summary:

- EXAFS fitting of model compounds indicates it is possible to identify and quantify four distinct classes of tungsten in soils: tungsten metal (absent), true tungstates (Class 2), tungstate minerals (Class 3), and polytungstates or POMs (Class 4).
- It is not possible to differentiate among specific POMs or some mineral phases based on linear combination fitting alone owing to their structural (and spectral) similarity.

4.1.2.5 Tungsten Speciation with Depth Using EXAFS

Extended X-ray absorption fine structure analysis spectra of the contaminated soil profiles revealed consistent changes in tungsten speciation with depth (Fig. 5). All samples, Profiles A and B, regardless of depth or location contained insignificant (5±7% or less) tungsten metal in agreement with XANES data. Profile A consists of composite soil samples (MMRBLB073B, MMRBLB074B, and MMRLB075B) collected from the lower berm of Bravo Range at Camp Edwards near Targets 23, 26, 30, and 34. The profile B sample was obtained from a single core in the trough on Bravo Range near Target no. 31 (samples MMRB0510 through MMRB5060). Additionally, crystalline tungstate minerals like $FeWO_4$ never represented a majority of tungsten in the soils, although it is clearly more prevalent than tungsten metal. In fact, in most samples, adsorbed polytungstates or other POMs, $H_3PW_{12}O_{40}$, appeared to be the dominant fraction of soil tungsten throughout the soil profiles. The fraction of adsorbed tungstate (Class 2, true tetrahedral WO_4^{2-} adsorbed to soil minerals) was also significant, and generally increased with soil depth (as the total tungsten concentration decreased).

However, because the total concentration of tungsten decreased with depth, adsorbed WO_4^{2-} concentrations do not appear to increase with depth. The increased prevalence of tungstate at depth, which is more stable in basic solutions, may reflect the neutral and slightly alkaline pH of deeper soil horizons, while polytungstates are more stable in acidic to slightly acidic conditions of surface soil horizons (Baes and Mesmer 1986; Koutsospyros et al. 2006).

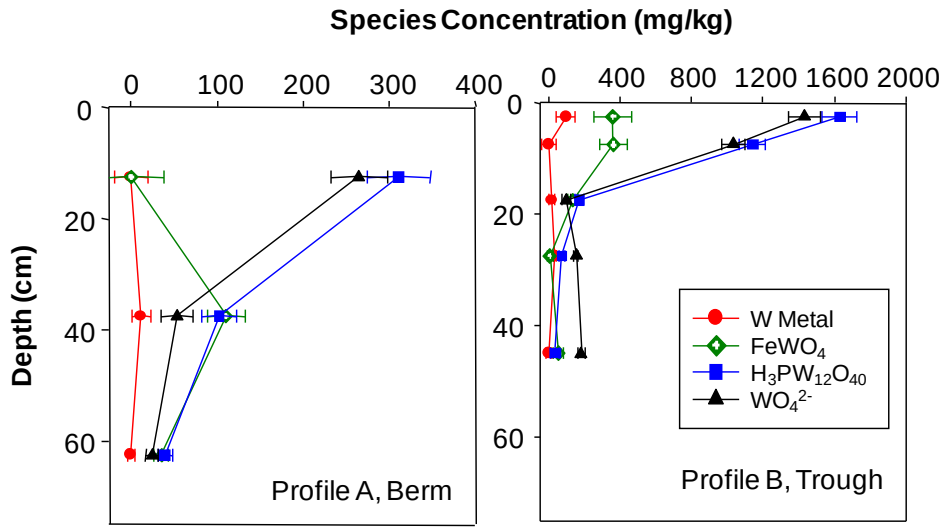

Figure 5. Changes in tungsten speciation with depth for soil profiles A and B from Camp Edwards.

In conjunction with the spectra of reference materials, it is possible to calculate the relative concentrations of component mineral (or other) phases in a soil sample. To do so, the EXAFS (or XANES) spectra of soil samples can be fit with fractional contributions of known reference spectra to calculate the fractional abundance of each component in the soil. This is done for a series of soils from the Camp Edwards site (MMRB0510 through MMRB5060) obtained from the trough of Bravo Range near Target no. 31 prior to soil removal. These spectra all have a similar spectrum, dominated by a single low frequency sine wave; this spectrum indicates a dominant W-O coordination environment (compare to spectra in Fig. 4) and clearly lacks features attributed to tungsten metal (Fig. 6). Tungsten metal would have a W-W shell resulting in a higher frequency pattern with a lot of interference (Fig. 4). In fact, little or no tungsten metal is needed to fit the experimental spectra accurately (Fig. 5), and polytungstates (Class 4 tungsten compounds) species are more prevalent than simple tungstate anions at all depths. This result is significant because it indicates, for the first time, such complexes form in soils, and they represent an appreciable fraction of adsorbed tungsten. Thus, an understanding of how these complexes form in soil systems and how they react with soil minerals is needed to accurately assess the fate of tungsten in soils.

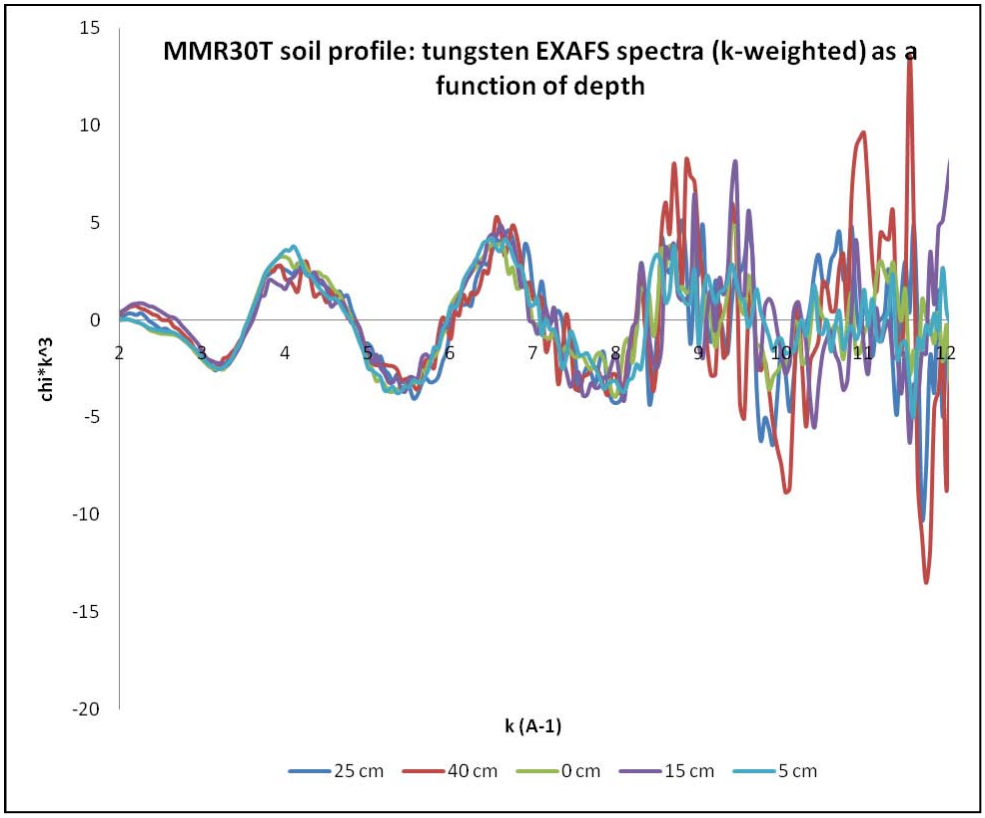

Figure 6. k^3-weighted tungsten L_3 EXAFS spectra of Camp Edwards soil profile 31T as a function of depth. The spectra all indicate that the primary coordination sphere of tungsten is dominated by oxygen at all depths, indicating extensive oxidation.

Linear combination fitting (Fig. 5) indicates polytungstates are common in soils, but it is unknown, based on the fitting, which polytungstates or POMs are present. To some extent, however, their separation is possible with theoretical fitting of tungsten spectra. Detailed theoretical fitting was performed on two Camp Edwards surface soils, Test MMRB05 obtained from the trough floor on Bravo Range near Target no. 31 and MMRBMB023S2 obtained from the middle berm region of Bravo Range, in an attempt to differentiate between conventional, homonuclear poly-tungstates (those containing only tungsten), and POMs (Table 3, Fig. 7). These soils were chosen on the basis of their high tungsten concentration (which improved data quality) and their linear combination fitting results, which implied that 50–70% of the tungsten was present as polytungstate or POM. Thus, spectral features attributed to specific polytungstates or POMS should be easily distinguished in spectrum of the soil, which re-flected the net spectrum of the soil mixture. In each case, spectral fitting (Table 3) matched the W-O and W-W shells of well characterized POMs (Table 2). Unfortunately, the spectra of both POM reference materials and these samples lack well defined P, Si, or other shells useful to distinguish

among different POMs because these features are masked by W-W shells. Nevertheless, the remarkably similar spectra of all of the examined soils suggest that POMs (rather than homonuclear polytungstates) may be important adsorbed species in these soils, although considerably more work is needed to conclusively identify the POM species in these soils.

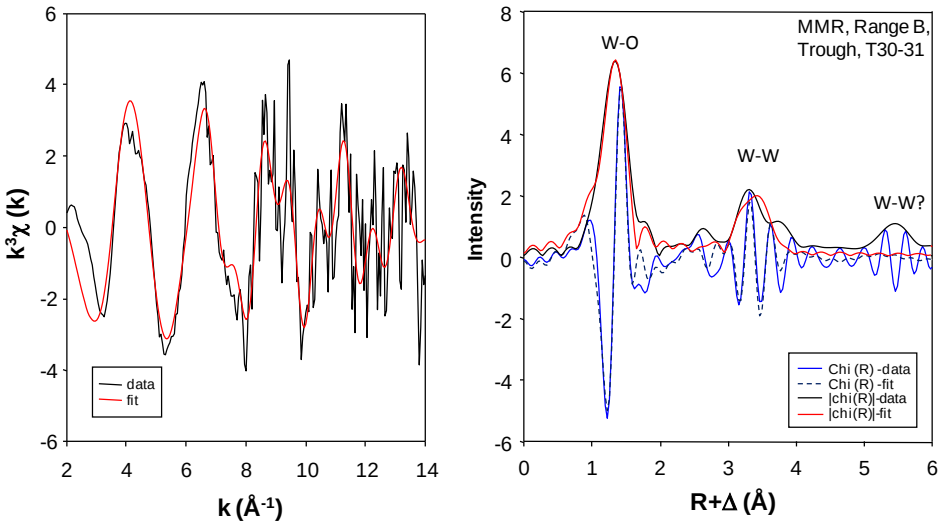

Figure 7. Detailed theoretical fits of W L_3-edge EXAFS spectra for a soil containing >50% POM or polytungstate based on least squares fitting. The fitting results are consistent with the prevalence of POMs in these soils. The close match of the spectrum (black lines) and the fit (red and dashed lines) are consistent with POMs of similar structure to the α-Keggin cluster.

Additional evidence for the presence of POMs is the known thermodynamic stability of polytungstates. Polytungstates are stable under acidic conditions, but are highly insoluble (net solubility is 1 mg L^{-1} or less under most conditions based on thermodynamic data for soil solutions at pH 7). POMs on the other hand, may be more stable at neutral conditions, and have different solubilities or adsorption behavior allowing them to be more conclusively identified based on those macroscopic properties.

The results of the EXAFS measurements can be summarized as follows:

- The speciation of tungsten is very complex, with tetrahedral tungstate, which is stable in alkaline solutions, converted to a variety of polytungstates in neutral and acidic pH solutions common to soils.
- Contaminated soils revealed changes in tungsten speciation with depth (decline of polytungstates and POMs), increased tungstate adsorption, and contained insignificant (5±7% or less) tungsten metal, consistent with XANES findings.

- Crystalline tungstate minerals such as $FeWO_4$ do not appear to represent a majority of tungsten in the soils.
- Adsorbed polytungstates or other POMs appeared to be the dominant tungsten fraction in shallow soil. The fraction of adsorbed tungstate was also significant and generally increased with soil depth while the fraction of polytungstate or POM, or both, decreased with increasing soil depth.

Table 3. EXAFS fitting parameters for select soil samples high in polytungstate.

Sample/ Fit quality	Shell	CN	R (Å)	σ^2 (Å^2)
Test 05	W-O	2[a]	1.75	0.002
MMR, Range B,	W-O	3[a]	1.92	0.007
Trough, T30-31	W-W	2[a]	3.39	0.007
X_{red}^2 = 6.72[b]	W-W	2[a]	3.70	0.008
B023S2	W-O	2[a]	1.74	0.003
MMR, Range B,	W-O	3[a]	1.93	0.008
Bullet pocket	W-W	2[a]	3.42	0.006
X_{red}^2 = 8.1[b]	W-W	2[a]	3.71	0.009

(a): Fixed during fitting based on crystallographic data.

(b): Reduced chi-squared of the fit.

– ——— , where ν is the degrees of freedom, X_{red}^2 is the observed value at a point, E is the modeled (expected) value, and σ^2 is the variance.

The coordination number (CN) is typically accurate to within ±1, interatomic distance (R) within ± 0.02 Å; σ^2 represents the variance in R (in Å^2). For all of the reference materials, E^0 was ≈ 10,207 eV.

4.1.3 X-Ray Microprobe Studies

X-ray microprobe studies are invaluable in determining the elemental abundance and phase associations of tungsten with other elements, and this information is useful for refining our understanding of which tungsten minerals are present, minerals that adsorb tungstate and POMs, and the dominant forms of tungsten in these soils.

The μXRF maps change considerably from soil depths of 0 to 20 cm, with contaminated surface soils appearing more heterogeneous than soils at depth (Fig. 8). The surface 0–5 cm of the soils (Fig. 8, upper left) contains zones of high iron, tungsten, and calcium counts (proportional to concen-

tration) separated from the bulk matrix. By 5–10 cm (Fig. 8, lower left), the regions of high tungsten counts (red) are no longer prominent, and tungsten appears to be relatively evenly distributed throughout the soil. This well-distributed tungsten is also found at the 15–20 cm depth (Fig. 8, lower right). In each map, normalized tungsten counts are positively correlated to iron counts (R^2=0.64 for the map of the 5–10 cm depth interval), although this linear correlation is not strong (R^2=0.21) for the surface soil sample (0–5 cm) because it had a relatively narrow range of concentrations, i.e., most samples exhibited very high tungsten values. At intermediate depths, the correlation contains two distinct populations: 1) very high tungsten concentrations grouped (but poorly correlated, R^2<0.2 for the group) to high iron levels, and 2) lower tungsten concentrations correlated to iron levels (R^2 =0.61). Overall, the correlation of iron and tungsten counts, or the association of high-tungsten with iron-enriched areas within the images, implies that much of the tungsten in the subsurface soil samples is adsorbed on iron minerals, presumably iron oxides.

Identification of adsorbed forms of tungstate was confirmed at a variety of points using micro-XANES spectroscopy (Fig. 9). Iron hotspots in the 0–5 cm depth interval had iron *K*-edge spectra, indicative of ferrihydrite, $Fe(OH)_3$, and, in one case, hematite, Fe_2O_3. Ferrihydrite is a high surface area iron oxide, and tungstate adsorbs strongly to its surface under normal conditions (Gustafsson 2003). In no cases were the XANES spectra indicative of ferberite, $FeWO_4$(s). Thus, although smaller quantities of this mineral may be present, it is not dominant, and adsorbed forms of tungsten (either tungstate or polytungstates) are the principal forms of tungsten in these soils. Tungsten XANES spectra can further determine if hotspots contain metallic tungsten, tungstates, or polytungstates. In each case, tungsten is present as tungsten(VI), tungstate, and polytungstate. Tungsten and iron XANES spectra in both tungsten and iron hotspots are indistinguishable—each is consistent with tungstate or polytungstates and ferrihydrite or other iron oxides. Thus, micro-XANES spectroscopy suggests most tungsten in this soil profile is one or more (poly)tungstates that are adsorbed primarily to ferrihydrite.

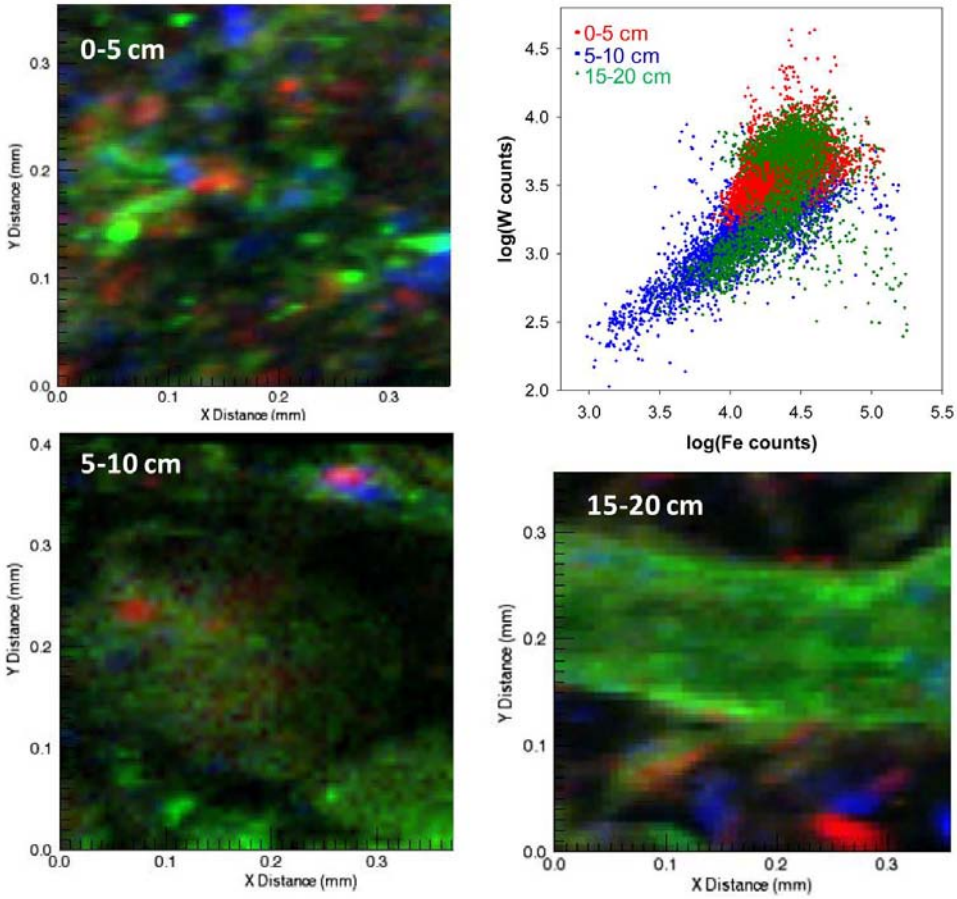

Figure 8. Microprobe XRF images of normalized iron (red), tungsten (green) and calcium (blue) fluorescence intensities for a soil collected from a trough area. Iron, calcium, and tungsten intensities in the surface soil contain numerous hotspots, but are not obviously collocated in the same grains. The correlation of log normalized iron and tungsten counts (upper right) is apparent in all samples, although it is strongest for the deeper soil samples with overall lower tungsten concentrations, and suggests adsorption of tungsten to iron phases. (Soil profile taken at Camp Edwards Range B, Trough 30-31.)

The presence of well defined, highly concentrated tungsten regions, particularly at the surface (Fig. 8), could result from the presence of tungsten-rich mineral phases, including WO_3, $CaWO_4$, or $FeWO_4$. Linear combination fitting also suggests that these mineral phases are present at this depth interval (Fig. 5). While some of these mineral phases may be present, μXRF indicates that iron hotspots are not $FeWO_4$ and does not identify any correlation between tungsten and calcium concentrations (R^2<0.1). Thus, small quantities of these minerals can form but do not appear to be dominant even in these soils.

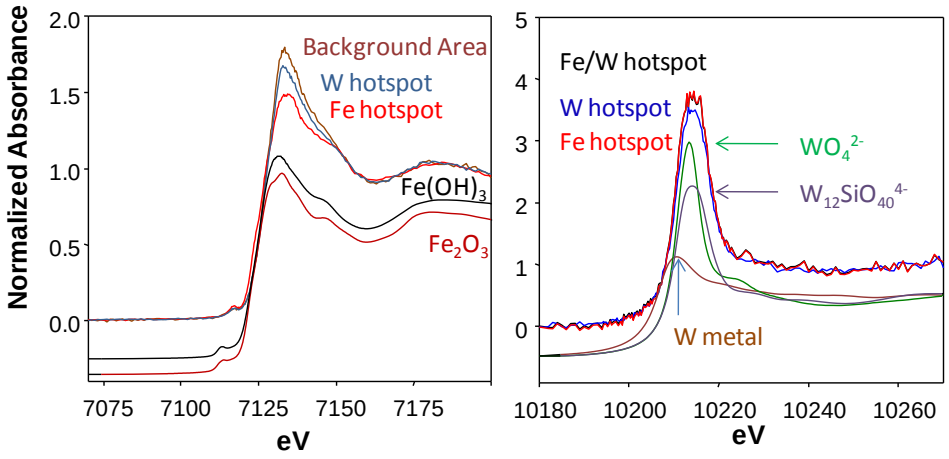

Figure 9. Microprobe iron (left) and tungsten XANES spectra (right) for representative iron and tungsten-rich spots in the XRF microprobe image in Figure 8. Selected iron and tungsten reference spectra are offset from the soils spectra for clarity. The iron spectra indicate that the iron is present as ferrihydrite and hematite, and the tungsten associated with both tungsten hotspots and background areas is a tungstate or polytungstate. (Soil sample: Camp Edwards Range B, Trough 30-31, 0-5 cm depth interval.)

Instead, tungsten-rich regions within the μXRF images appear to result from the association of high concentrations of adsorbed tungstate to reactive iron phases. These high-tungsten points also overlie the iron–tungsten correlation observed at depth, and these tungsten hotspots may just be soil aggregates with high-surface areas containing iron oxides.

Tungsten also could adsorb on other minerals, including manganese oxides, silicates, and other phases. The lack of correlation between tungsten and manganese counts implies manganese oxides are not major adsorbents of tungstate, at least in these soils. It is not possible to accurately measure aluminum or silicate counts on this beam line as configured, so it is not possible to determine the potential role of aluminosilicates for tungstate retention; however, it is expected to be relatively minor because these soils have relatively low clay contents and coarse sands have low surface areas.

To summarize:

- Surface soils between 0–5 cm contain zones of high iron, tungsten, and calcium counts from the bulk matrix. By the 5–10 cm depth interval, regions of high tungsten density associated with increased adsorption are no longer prominent, and tungsten appears to be relatively evenly distributed throughout the soil. The lower tungsten densities with

depth appear to be associated with a lack of available adsorption sites as discussed in earlier.

- Tungstates are likely adsorbed primarily to ferrihydrite and are not correlated to calcium, manganese, silicon, or aluminum in these soils, suggesting lack of covalently bonded tungsten in crystalline phases.

4.1.4 Apparent Solubility of Soil Tungsten

Based on spectroscopic results, we find that most of the tungsten in these soils is present in adsorbed forms. As such, the stability and transport properties of tungsten in soil systems should depend strongly on the relative adsorption affinity of these adsorbed forms for common soil minerals, particularly iron oxides. To further establish that adsorbed species are present, and to determine the affinity of these complexes for mineral surfaces, a series of desorption isotherms were calculated using the soils equilibrated with various volumes of water (Appendix A). These desorption isotherms for a typical contaminated soil at the site (MMRBMB036S3, which had a moderate tungsten concentration of 1626±450 mg kg^{-1}) exhibited significant desorption, approximately 10% of the tungsten desorbed, with solution tungsten concentrations reaching more than 5500 mg L^{-1} (Fig. 10A). At these high concentrations, the effective partition coefficient (K_d) was only 0.2 L kg^{-1}(eq1 and 2). Across all soils at a single solid–solution ratio, desorption also followed a similar pattern (Fig. 10B), with aqueous concentrations in some cases reaching 1500 mg L^{-1}. The considerable scatter in adsorbed tungstate concentrations is most likely caused by the variability in iron concentrations. As spectral data indicate that iron oxides are important adsorbents of tungstate, their presence should affect adsorption and thereby aqueous tungsten concentrations. To test this, we can normalize solid-phase tungsten concentrations to iron content (Fig. 10C). Indeed, much of the variation in adsorption across all soils appears to relate to differences in the iron content of the soils (Fig. 10C). Soils from the Camp Edwards site, in particular, are well described by a single isotherm, likely because of their overall similar soil properties.

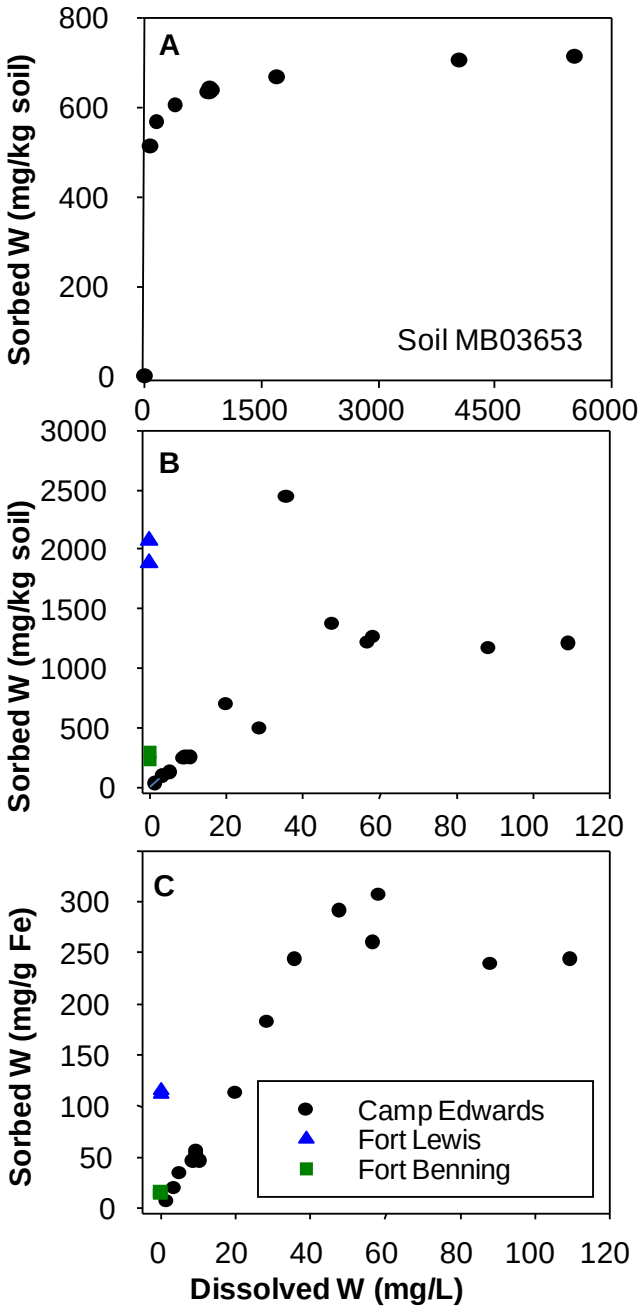

Figure 10. Desorption isotherms for soil sample MMRBMB036S3 (A) at a range of solid-solution ratios, and for all soils (B) at a fixed solid solution ratio. Accounting for variable iron concentrations in the soils (C) suggests a single isotherm, or iron oxides, control adsorption in Camp Edwards soils. The equilibrium pH for the soil sample MMRBMB036S3 is about pH 6.4 and ranges from 6–7 for most soils from Camp Edwards, and 5–6 for the Northwest and Southeast Site soils.

We can glean a considerable amount of information about what regulates tungsten concentrations in soils using the shape of adsorption or desorption isotherms. The isotherms in Figures 10A, B, and C have shapes characteristic of nonlinear adsorption phenomena, with a clearly defined adsorption maximum (or nearly so) and no apparent limits to dissolved tungsten concentrations. In contrast, if mineral dissolution controlled tungsten solubility, concentrations would be relatively uniform and limited by the concentration of one or more additional elements (for example Ca^{2+} concentrations for a $CaWO_4$ mineral). The desorption isotherms fit to both Langmuir and Freundlich equations utilizing a least-squares approach, although Freundlich isotherms yielded slightly better fits (Fig. 11). While the adsorption maxima were reasonably high, the partition coefficient, and Langmuir or Freundlich adsorption constants calculated for the desorption isotherms, all were consistent with very weak tungsten adsorption at high concentrations, consistent with the field observation of tungsten being present in groundwater at Camp Edwards (Clausen et al. 2007, 2010). Similarly weak adsorption has been observed in other contaminated sites, particularly those containing munitions (Dermatas et al. 2004; Bednar et al. 2008; Clausen et al. 2010).

Langmuir equation:

$$\Gamma = \frac{\Gamma_{max} K_L C}{1 + K_L C} = \frac{672 \times 0.034 C}{1 + 0.034 C} \quad (1)$$

Where

Γ = amount of material adsorbed (mL g^{-1})
Γ_{max} = maximum amount of material adsorbed (mg kg^{-1})
K_L = Langmuir equilibrium constant (L mg^{-1})
C = equilibrium aqueous concentration of adsorbate in solution (mg/L).

Freundlich equation:

$$\Gamma = K_F C^{\frac{1}{n}} = 379 \frac{1}{13.25} \quad (2)$$

Where

Γ = amount of material adsorbed (mL g^{-1})
n = constant (unitless)

K_F = Freundlich equilibrium constant (L mg^{-1})
C = equilibrium aqueous concentration of adsorbate in solution (mg L^{-1}).

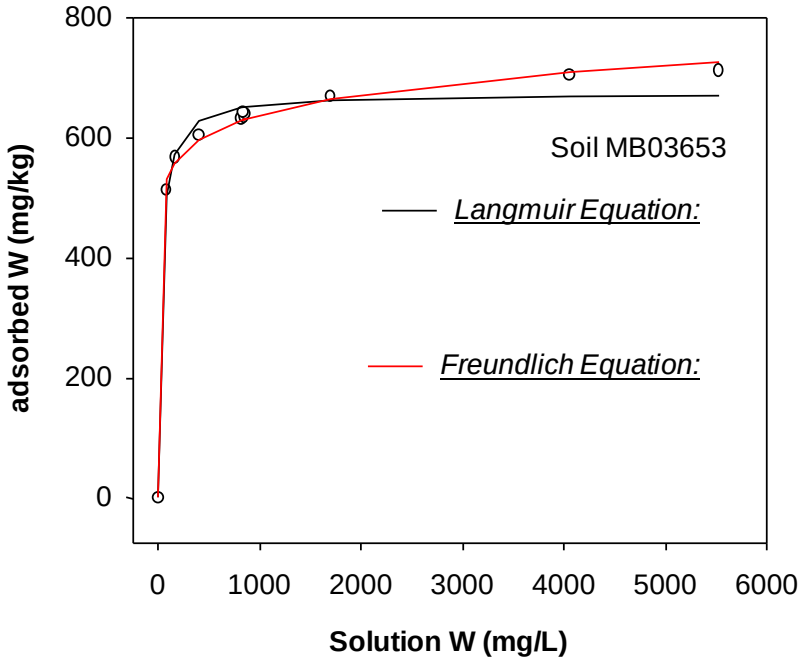

Figure 11. Langmuir and Freundlich isotherms derived for desorption experiments for soil sample MMRBMB036S3.

The soils from Southeast Site and Northwest Site have stronger adsorption than those at Camp Edwards, as evidenced by their relatively high solid-phase tungsten concentration and very slight tungsten release during desorption experiments (Fig. 10). The lower solubility of tungsten in Southeast Site and Northwest Site soils may be the result of their lower pH (their pH is 5 to 6) and higher iron oxide content as compared to the Camp Edwards soils. Tungstate is more strongly adsorbed to ferrihydrite at lower pH (Gustafsson 2003) and these soils have considerably more iron on which to adsorb. Thus, tungsten would be expected to be less susceptible to leaching losses in these soils. It is also possible differences may be attributable to the concentration of P in the soil; however, this analyte was not determined in these soils. The Camp Edwards soil was treated with MAECTITE, a P-base material. Therefore, it is likely that the Camp Edwards soil has a higher P content than the Southeast Site and Northwest Site soils. Coupled with a lower initial tungsten soil content (Clausen and Korte 2009), the speciation findings are consistent with a considerably lower amount of tungsten observed in lysimeters monitoring subsurface

soil pore water from the Southeast and Northwest sites as compared to Camp Edwards.

As shown in the Phase II tungsten work (Clausen et al. 2010), sorption was time dependent with increasing equilibration time resulting in increasing K_d values. Although the desorption and adsorption experiments are instructive in understanding tungsten behavior, relying on calculated K_d values for transport determinations is not recommended, as it is unclear whether the experimental conditions represent field conditions. For example, the equilibration interval of 24-hours used in the experiments is likely shorter than the contact time of tungsten with site soils.

To summarize:

- Adsorption and desorption of tungsten depends on available iron and its distribution for Camp Edwards soil.
- Significant desorption of tungsten is apparent for Camp Edwards soil and the isotherm can be fit with both Langmuir and Freundlich equations.
- At high concentrations tungsten is weakly adsorbed, which is probably a function of filled adsorption sites.
- Soils from the Southeast and Northwest sites adsorbed tungsten to a greater extent and were less likely to desorb tungsten than Camp Edwards soils owing to their higher iron content.
- One of the most striking results of the desorption experiments is that the concentration of tungsten in the aqueous phase reached very high values (>1000 mg L^{-1}). These high concentrations are vastly in excess of theoretical limits based on the solubility of tungstate minerals calculated by Visual Minteq (or other programs), and indicates tungsten is stabilized in solution much more than is currently recognized. This high solubility is most important in highly contaminated soils and represents a very important factor to consider in managing tungsten-impacted sites.

4.1.5 Possible Explanation for the High Solubility of Tungsten

Little information is available in the literature to corroborate and explain the adsorption behavior of tungsten in natural systems. Tungstate adsorption isotherms look qualitatively similar to those on goethite (Xu et al. 2006) and ferrihydrite (Gustafsson 2003). However, the weak tungstate retention observed in our experiments differs considerably from the rela-

tively strong adsorption behavior observed with these model systems. In fact, Gustafsson (2003) suggests tungstate adsorption is sufficiently strong to displace phosphate (a very strong adsorbent) from adsorption sites. It seems clear that tungstate is not displacing the P added (MAECTITE™) in the Camp Edwards soil (Clausen et al. 2010). This strong adsorption is related to the formation of stable tungstate surface complexes on the mineral surface—eq 3 and 4 (Gustafsson 2003):

$$\equiv FeOH^{-0.5} + WO^{\frac{2-}{4}} + H_2O + 2H^+ \Leftrightarrow \equiv Fe - OWOH_5^{-0.5}, \text{ Log } K = 19.35 \quad (3)$$

$$\equiv FeOH^{-0.5} + H^+ + H + WO_4^{2-} \Leftrightarrow \equiv Fe - OWO_3^{-0.5} + H_2O, \text{ Log } K = 14.07 \quad (4)$$

Equations 3 and 4 are derived based on measured W(VI) adsorption and use the measured solution speciation of tungsten and its adsorption in simple solutions (predominantly those containing only tungsten and background electrolytes). In general, eq 3 is favored at pH<6, while tungstate adsorption (eq 4) is more significant at neutral and higher pH, although total tungstate adsorption diminishes at pH>8 (Xu et al. 2006).

The exceptional solubility of tungstate in the soils used in this study is considerably altered by the presence of other ions in soil solutions. These ions can react with the surface independently, or influence tungsten speciation in solution and thereby indirectly influence tungsten retention. The small arms range berm soils in question at Camp Edwards were previously treated with MAECTITE™, a phosphate based proprietary material used to bind lead. This material may have filled all of the available adsorption sites, thus preventing or limiting tungsten's sorption despite its theoretical ability to displace phosphate (Clausen et al. 2010). The adsorption of other ions to the surface results in competition for the surface, which will affect tungsten adsorption, particularly if other ions react more strongly than tungstate, or are found at high concentrations. For example, tungstate adsorption influences molybdate adsorption appreciably because molybdate is adsorbed less strongly than tungstate, and the equilibria quantify this inhibition quite effectively (Xu et al. 2006). Soil solutions are complex, containing a number of possible species that could compete with tungstate adsorption, including molybdate, silicate, and carbonate, among others. Although competition undoubtedly does affect tungstate retention, the adsorption affinity or concentrations of potential competing ions are insufficient to yield measurable effects (Xu et al. 2006). Thus, the soil solution

must affect tungsten speciation in other ways. The precipitation of soil minerals also would limit tungsten concentrations below observed values, and tungsten oxides and $CaWO_4$ are both thermodynamically unstable (as indicated by the saturation indices, calculated for 100 mg L^{-1} total tungstate) except at very high tungsten concentrations in these soil solutions (Table 4).

Table 4. Solution composition and saturation indices for selected minerals for equilibrated waters from desorption experiments.

Ion	Total Concentration (mg L^{-1})[a]	Mineral	SI[b]
WO_4^{2-}	100–5,500		
Al^{3+}	0.02	W_{tot}=100 mg/L, Ca=110 mg/L	
AsO_4^{3-}	0.002	Scheelite ($CaWO_4$)	2.26
Ba^{2+}	0.02	$WO_3.H_2O$	–1.4
Ca^{2+}	12–110		
Fe^{2+}	0.05	W_{tot}=100 mg/L, Ca=12 mg/L	
$K^{+`}$	1.5	Scheelite ($CaWO_4$)	1.53
Li^{+}	0.001	$WO_3.H_2O$	–1.1
Mg^{2+}	2.0		
Mn^{2+}	0.001	W_{tot}=5500 mg/L, Ca=110 mg/L	
Na^{+}	25	Scheelite ($CaWO_4$)	2.8©
PO_4^{3-}5–75	$WO_3.H_2O$		–0.4[c]
SO_4^{2-}	0–2–5		
Sr^{2+}	0.04		
Zn^{2+}	0.1		

(a) Total concentration for the pore water following equilibration with the soil. In a few cases, the solid-solution ratio influenced the final ion concentrations. In these cases, the range reported reflects the total range in concentrations, with the concentration of the high solid-solution ratios reported first.

(b) The saturation index. $SI = \log\left(\frac{IAP}{K_{sp}}\right)$ where *IAP* is the ion activity product for the formation of the soil, and K_{sp} is the saturation index.

(c) The calculated ionic strength is very high owing to the high tungsten concentration. This result is some-what unreliable because the activity coefficients are difficult to calculate for such solutions.

The equilibrium pH was about 6.5±0.2.

The incorporation of tungstate into POMs would also affect the extent of tungstate adsorption by decreasing the fraction of free tungstate in solution. Soils have high concentrations of a number of species suitable for such incorporation in POMs, including P^{5+}, Si^{4+}, B, Zn^{2+}, and V^{3+} (Chen et

al. 2004). Of these, P^{5+} and Si^{4+} both are present in high concentrations in soil solutions and form Keggin clusters through the condensation of tungstate (eq 5 and 6):

$$12WO_4^{2-} + Si(OH)^4 + 20H^+ \Leftrightarrow W_{12}SiO_{40}^{4-} + 12H_2O \quad (5)$$

$$12WO_4^{2-} + PO_4^{3-} + 24H^+ \Leftrightarrow W_{12}PO_{40}^{4-} + 12H_2O \quad (6)$$

Although these complexes are well known, there is no information about their thermodynamic stability, so it is not possible to evaluate their prevalence in solution. However, empirical data from our studies suggest these species, in particular, are in fact present and presumably in other soil systems. First, spectral data established the presence of polytungstates in soils with pH >6.5, conditions in which the predicted solution speciation is dominated by WO_4^{2-}. In fact, spectra with high fractions of polytungstates have spectral features attributable to POMs specifically (Fig. 6), although such studies are not able to resolve shells attributed to heteroatoms, such as Si or P, because of the presence of intense W-W shells at similar distances.

An important piece of information regarding adsorption comes from the solution concentrations of tungsten in the desorption experiments. The high concentrations of tungsten from desorption experiments exceed known mineral solubilities, yet they represent minimum concentrations because additional reaction time would only result in additional dissolution. Consequently, disequilibrium processes such as a lack of mineral precipitation or slow adsorption cannot explain high solution concentrations. The desorption experiments, performed at pH 6.5, contained ~2 mM Ca^{2+} (Table 4). For all desorption experiments, tungsten concentrations ranged between 180–5500 mg L^{-1} (Appendix A). At these conditions, $CaWO_{4(s)}$ is supersaturated (W saturation is achieved at about ~1 mg L^{-1}). Thus, mineral forms of tungsten should remove tungsten from solution and impart a limit on tungsten concentrations (as long as there is adequate Ca^{2+} or other cations available in the soil solution), and mineral forms of tungstate would not dissolve in desorption experiments. So, these minerals cannot regulate tungsten levels, at least in these soils, and other factors must enhance tungsten solubility.

The stabilization of tungsten in solution, however, would allow solution concentrations to increase in response to weak adsorption. The reaction of

dissolved species with tungstate could strongly influence the stability of tungsten in soil solutions. For example, calcium and magnesium each form tungstate complexes ($CaWO_4^0$ and $MgWO_4^0$). Based on their known stability constants (log K = 2.57 and 3.03 for the formation of the complexes from WO_4^{2-} respectively), these complexes would decrease the concentration of free tungstate by about a factor of two, thereby increasing the solubility of tungsten in solution by about the same factor. Because soil solutions contain both Ca and Mg (Appendix A), these complexes are probably important in the environment, but they alone are not sufficiently stable to change the concentration of aqueous tungsten significantly. Thus, other solution complexes are needed to describe tungsten partitioning in more concentrated tungsten solutions.

The formation of aqueous POMs, which is supported by the spectral data, also would impact adsorption. Adsorption experiments were used to evaluate the possible formation of $W_{12}SiW_{40}^{4-}$, a model POM, to establish whether such complexes would influence tungsten adsorption. Adsorption isotherms (pH 7) of tungstate alone on ferrihydrite were similar to others in the literature (Xu et al. 2006). Appreciable adsorption occurred up to an adsorption maximum of 8 μmol m^{-2}, with solutions containing up to 10 mg L^{-1} tungstates (Fig. 12). The partition coefficient was approximately 40 L kg^{-1} at the adsorption maximum. The extent of tungsten adsorption changed considerably when Si was added to the system. Small quantities of Si (to an initial concentration of 1 mg L^{-1}) drastically decreased tungstate adsorption. In fact, this small concentration of dissolved Si, which is similar to that of the desorption experiments, was sufficient to decrease the magnitude of the partition coefficient to 1 or less (no significant tungsten adsorption, within the error of the measurement). This added Si would also be expected to adsorb to the solids, but is not of sufficient concentration to affect tungstate adsorption by competitive adsorption. It is, however, sufficient to convert all of the tungstate in solution to $W_{12}SiO_{40}^4$.

Thus, the effect of Si on adsorption is not from competitive adsorption and must result from its effect on tungsten speciation. Adsorption experiments were devoid of calcium or magnesium, both of which could influence WO_4 adsorption by forming stable solution complexes. Given that Si impedes adsorption so effectively in the absence of these ions, calcium and magnesium complexes do not appear to be required to influence adsorption. Experiments were not conducted to explore the relationship of P to adsorp-

tion. However, Bednar et al. (2008) assessed the impacts of this analyte and found that P could foster the formation of tungstate complexes, which will influence the degree of adsorption.

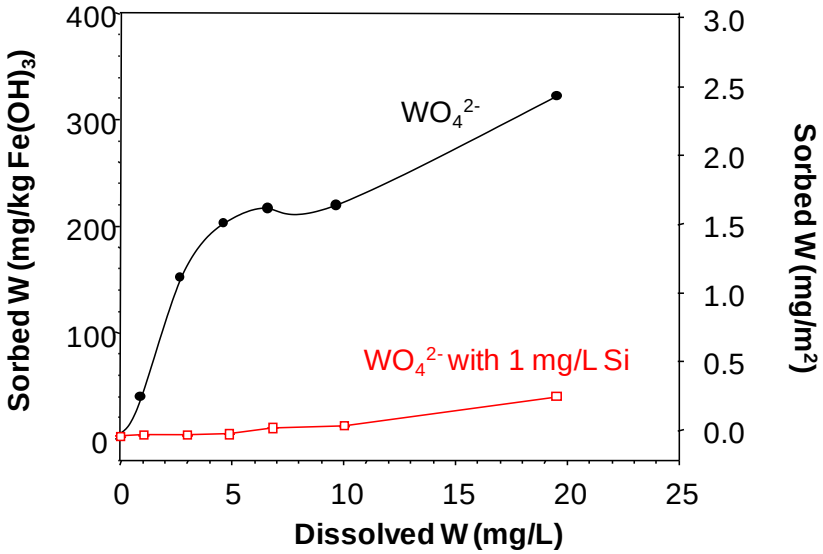

Figure 12. Adsorption isotherms for tungstate solutions (0–20 mg L^{-1}) in equilibrium with ferrihydrite (1 g L^{-1}). The addition of Si significantly diminished adsorption. The two *y*-axes apply to both lines—the left axis refers to the adsorbed tungsten in units of mass per mass, while the right axis shows adsorption in surface-area normalized units.

To summarize:

- Very high tungsten solution concentrations were observed in batch experiments, presumably because of filled adsorption sites.
- Ions present in soil solution can influence tungsten concentration and the degree of adsorption, as can the incorporation of tungstate into POMs.
- Increased Si concentrations decreased tungsten adsorption.
- The MAECTITE™ P material used to remediate lead in the Camp Edwards SAR berms may be responsible for tungsten's apparent increased mobility by preventing or limiting adsorption.

4.2 Tungsten Speciation in Water

The tungsten species present in pore-water solutions at Camp Edwards were explored using a newly developed analytical technique that separates tungsten species with size exclusion chromatography (SEC) followed by quantification with ICP-MS (Bednar et al. 2009). The method has a detec-

tion limit of 0.4 μg L^{-1} for tungstate. To resolve other species, however, higher concentrations are preferred, e.g., >1 to 1 ug/L. An earlier HPLC-ICP-MS method developed by Bednar et al. (2007) yields only semi-quantitative results. Unfortunately, this was the only method available in 2007 and was used to analyze water samples from MW-72S. Subsequent groundwater samples collected in 2009 had insufficient levels of tungsten to use the SEC-ICP-MS method and the original 2007 samples were no longer available for analysis. The concentrations of poly- and heteropoly-tungstates, as a group, can only be semi-quantitatively determined with the HPLC-ICP-MS method because they interact to some extent with the anion exchange column. In addition, resolving the speciation of tungsten requires comparison with analytical standards, which are not available for all of the species that may be present. The only standards available for comparison were sodium tungstate and polytungstate; the latter is listed as having the following composition: $Na_6[H_2W_{12}O_{40}]$ or $3Na_2WO_4 \cdot + 9WO_3 \cdot H_2O$. As noted above, polytungstates can be very complex, such that the species in the standard may not be the same as the species in the soil solution.

Outdoor dissolution tests conducted by (Clausen et al. 2010) with tungsten metal fragments suggest the production of both tungstate and poly-tungstate species in the water contacting the tungstate particles (Table 5). The results suggest polymerization is occurring directly on the tungsten metal surface and may be independent from the presence of soil (Clausen and Korte 2009, Clausen et al. 2010). It is also possible polymerization is occurring on both the tungsten metal surface as well as in the soil pore water.

The samples from the outdoor dissolution test yielded tungstate-to-polytungstate ratios of 11:1 to 19:1 (Table 5). This compares to lysimeter ratios of 4:1 to 14:1. The lower ratios from the lysimeters suggest preferential sorption of tungstate relative to polytungstate on a mass basis as compared to the dissolution tests. The ratios for lysimeters MMR-21 and MMR-30 appear relatively consistent over time.

Column test results (Clausen et al. 2010) also appear to yield higher tungstate to polytungstate ratios than those observed in the lysimeters (Table 5). However, so little polytungstate was present in the column test samples that analytical inaccuracies may affect these ratios. If the differences in ratios between the lysimeters and the column tests are real they

may be attributable to differences in degrees of saturation of the samples. The soil in the field probably oscillates between unsaturated and saturated conditions, with unsaturated conditions being more prevalent; whereas, the soil in the column tests largely remained saturated throughout the duration of the tests. As discussed previously (Clausen et al. 2010), polytungstate was not observed in the groundwater samples from MW-72S obtained on different sampling dates, possibly suggesting that polytungstate is eventually being attenuated in the Camp Edwards soil. However, as noted previously, the more sensitive SEC-ICP-MS wasn't available at the time the MW-72S sample was analyzed and subsequent samples had too little tungsten to use this method. The HPLC-ICP-MS method may have been too insensitive to see any polytungstate in the MW-72S groundwater sample.

Water samples remaining from the desorption test conducted during Phase II (Clausen et al. 2010) were analyzed with the SEC-ICP-MS method. The tungstate to polytungstate ratios for the desorption experiments conducted with sand, kaolinite clay, and goethite were largely similar to the lysimeter results (Table 5). In contrast, a much higher tungstate-to-polytungstate ratio was observed for peat, which is rich in organic matter. These results suggest the preferential sorption of polytungstate to the peat and, therefore, organic rich environments may impede the migration of polytungstates as compared to the soil conditions at Camp Edwards.

Shallow groundwater and surface water can be expected to have both tungstate and polytungstate species present. As shown above, the prevalence of tungstate versus polytungstate is variable and depends on soil conditions and the contact time (depth and migration rate). The geochemical conditions likely control the tungsten complexes formed, the degree of adsorption, and polymerization. The variables involved influencing the formation of tungstate versus polytungstate include pH level, iron, calcium, P, Si, and organic content of the soil and water, as well as depth of interest and migration rate of the water.

Table 5. Total tungsten measurements with ICP-MS compared to tungstate and polytungstate measurements using SEC-ICP-MS for batch and column test samples.

Lab Sample Id	Tungstate SEC-ICP-MS (µg L^{-1})	Polytung-state SEC-ICP-MS (µg L^{-1})	Ratio of Tungstate to Polytungstate	Total Recov-ery (%)	ICP-MS (µg L^{-1})	Comment
W100	67	4	17:1	71		QA/QC Standard, 100ug/L total tungsten
Blank	<1	<1	NA			
8061701-01	6,290	558	11:1		11,400	Outdoor dissolution Test 31W sample from 6/16/08
8061701-02	7,250	380	19:1		5,500	Outdoor dissolution Test 32W sample from 6/16/08
8062701-25	110	<10	NA		369	Column Test no. 1, 2B-297 sample, closest ICP sample no. 247
8062701-43	223	<10	NA		171	Column Test no. 2, 4A-49 sample, closest ICP sample no. 48
8071501-69	347	7 J	50:1		483	Column test no. 3, 4B-189 sample
8062701-05	<10	<10	NA		6.54	Batch test Substrate sample 1d of 6/6/08 with aluminum powder
8062701-05r	<10	<10	NA		6.54	Substrate sample 1d replicate of 6/6/08
8062701-05a	55	27	2:1	87.1		QA/QC Matrix spike sample of 1d, 100 µg/L total tungsten
8062701-49	3,220	1,190	3:1		2760	Batch test Substrate sample 5d of 6/6/08 with kaolinite clay
8062701-57	863	309	3:1		632	Batch test Substrate sample 9d of 6/6/08 with goethite (Mn rich)
8062701-63	1,130	65	17:1		1,240	Batch test Substrate sample 12d of 6/6/08 with peat
8062701-69	419	92	5:1		521	Batch test Substrate sample 15d of 6/6/08 with sand

J – Estimated value, NA – not applicable, QA/QC – quality assurance/quality control

Lysimeter MMR-30, located on Bravo Range, was installed on the berm face at a depth of 4.6 m below the ground surface. MMR-30 was sampled on 30 May and 19 December 2007. The response curves for the lysimeter samples (Fig. 13) compare favorably to the curves for the polytungstate and tungstate standards, indicating that both species are present. Re-

ported total tungsten concentrations by ICP-MS can be compared to the tungstate and polytungstate values obtained with the HPLC-ICP-MS separation (Table 6). The "total" tungsten values by ICP-MS tended to be lower than the tungstate + polytungstate results by HPLC-ICP-MS. The concentrations differ because, at the time of these analyses, the HPLC-ICP-MS method was semi-quantitative. The later improvement utilizing SEC-ICP-MS (Bednar et al. 2009) allows for increased quantitative precision; however, this technique was not developed at the time of the analysis in Figure 13. It is also possible that ageing of the sample may have led to further speciation changes, precipitation, or dissolution of tungsten from associated soil particles in the samples.

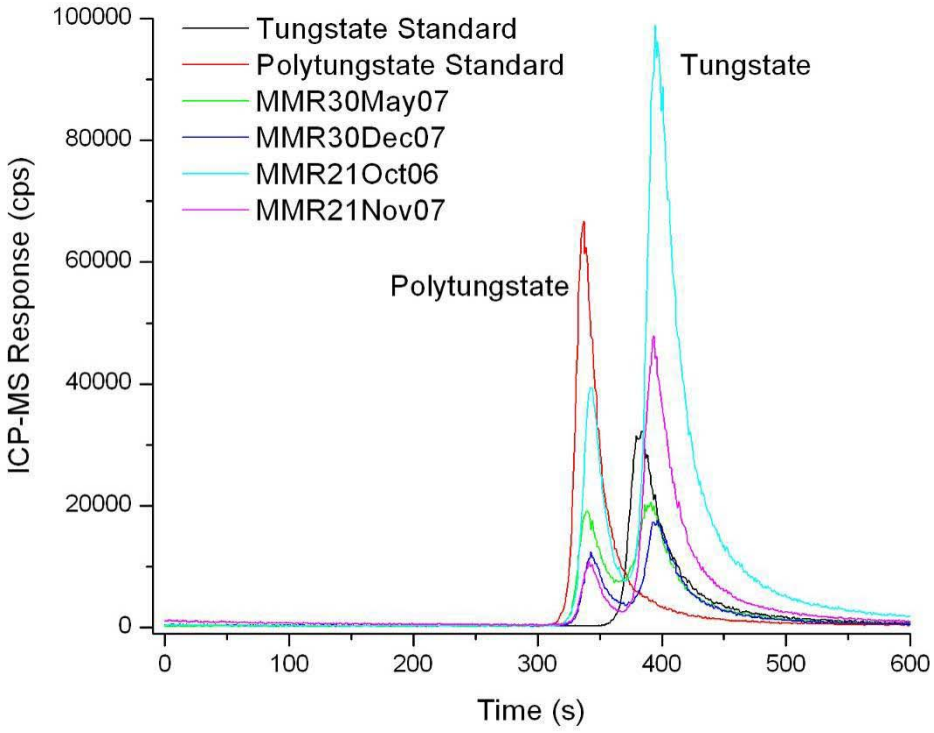

Figure 13. Speciation of tungsten in lysimeter samples from MMR-21 and MMR-30 using SEC-ICP-MS.

The lysimeter results suggest that the predominant species of tungsten present in the vadose zone at Camp Edwards is tungstate. However, the presence of polytungstate in the lysimeter samples described above shows that polymerization occurs in the vadose zone. There is a slight decrease in the tungsate:polytungstate ratios for MMR-21 vs. MMR-30, the latter approximately 3 m deeper than the former. As polytungstate is weakly sorbed to most soils, the decline in tungstate concentration in the vadose

zone pore water must be attributable to tungstate adsorption. Polymerization of tungstate is not a likely mechanism because increased polytungstate solution concentrations would result from the polytungstate being weakly sorbed to soil. Consequently, these results seem to suggest that tungstate is preferentially attenuated relative to polytungstate, which is opposite of the Bednar et al. (2008) observations.

Table 6. Total tungsten concentration compared to tungstate and polytungstate in Lysimeters MMR-21 and -30.

Lysimeter ID	Sample Date	Species Concentration (µg L^{-1})			
		Total Tungsten (ICP)	Tungstate (SEC-ICP-MS)	Polytungstate (SEC-ICP-MS)	Ratio of Tungstate to Polytungstate
MMR-21	October 2006	18,100	30,400	3,600	8:1
MMR-21	November 2007	10,000	14,100	980	14:1
MMR-30	May 2007	1,400	1,530	390	4:1
MMR-30	December 2007	1,400	1,170	230	6:1

As reported previously in Clausen et al. (2007), a sample from monitoring well MW-72S was analyzed for tungsten using the HPLC-ICP-MS speciation method of Bednar et al. (2007). The results for this particular sample were a good match with the sodium tungstate standard, with polytungstate species not being evident. This sample, collected on 10 May 2006, had a reported tungsten concentration of approximately 0.550 mg L^{-1} using ICP-MS.

Evaluation of water from MW-72S (Fig. 14) seems to suggest that polytungstates may not migrate as readily as tungstate, with attenuation occurring between 4.5 m and the 36-m deep water table. This is in contrast to the XAS soil work, which showed weak adsorption of polytungstate to Camp Edwards soil. However, it is possible that the difference between soil and water results can be explained by depolymerization that should occur at lower concentrations, although the threshold concentration required for depolymerization of complex polytungstates is not known, and the kinetics of tungstate-polytungstate equilibria are sufficiently slow (Koutsospyros et al. 2006), Therefore, it is difficult to conclude, based on the available data, how depolymerization affects transport. It is also possible that the HPLC-ICP-MS method was not particularly sensitive to polytungstate species

present in the MW-72S sample and that polytungstate is present in the groundwater. Unfortunately, insufficient sample is available to be tested with the more sensitive SEC-ICP-MS and the current tungsten concentrations in MW-72S, less than 2 ppb, are below the sensitivity of the new method. Therefore, it is possible that polytungstates were present in MW-72S but not detectable with method available at the time. In any event, the working conceptual model of tungsten concentration with depth is presented in Figure 15.

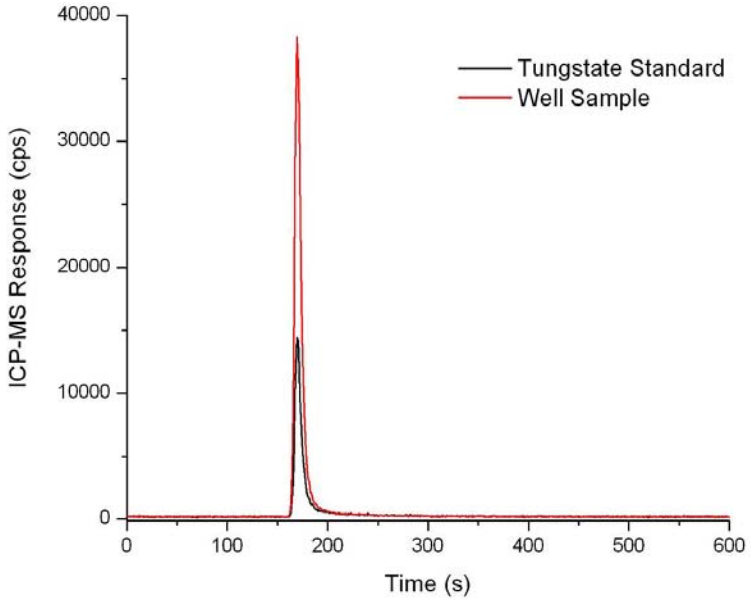

Figure 14. Speciation of tungsten in monitoring well sample MMR-72S using HPLC-ICP-MS.

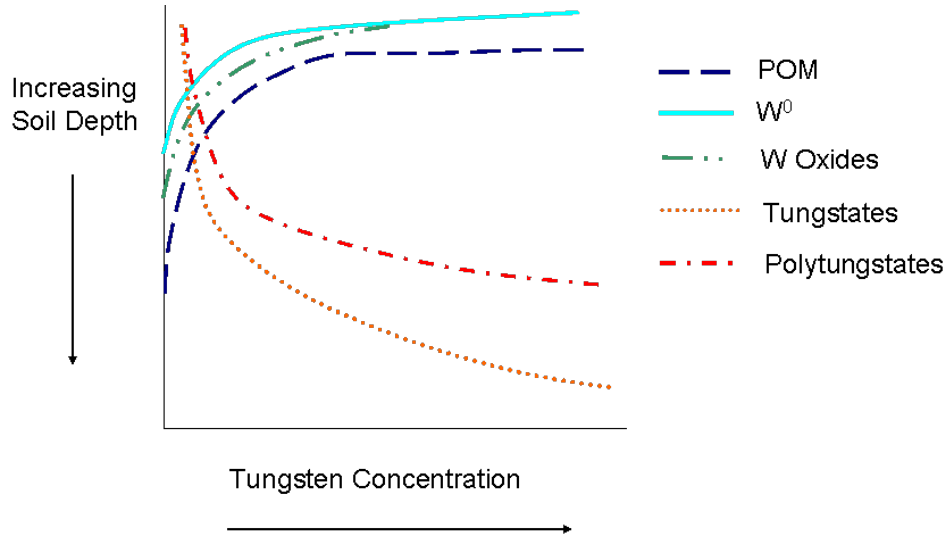

Figure 15. Relationship between tungsten concentration and soil depth.

In summary, the following observations are evident for tungsten in water:

- Dissolution tests with tungsten metal produce tungstate and polytungstate species.
- Tungstate and polytungstate species are present in vadose zone soil pore water at Camp Edwards and, although not specifically identified, POMs are also a possibility.
- The ratio of tungstate to polytungstate appears to decrease with increasing vadose zone depth, suggesting tungstate is adsorbed to a greater degree than polytungstate or the tungstate continues to undergo polymerization, increasing the amount of polytungstate and decreasing the amount of tungstate. However, if the latter were occurring, the polytungstates would have to be adsorbed to the soil. XAS data suggest polytungstates are the dominant tungsten form in soil. POMs were not specifically detected in the water, so the ratio with tungstate and polytungstate is not determinable.
- Ratios of tungstate to polytungstate in field lysimeters are relatively constant over time.
- Polytungstate was not detected in groundwater samples from MW-72S; however, the analytical method used at the time HPLC-ICP-MS may not have been sensitive enough for detection.
- Laboratory studies suggest polytungstate is preferentially sorbed to organic rich soils, impeding migration. Desorption experimental results were unclear and the tests would need to be repeated to determine the degree of desorption from organic rich soils.
- These site-specific results have broad implications for tungsten environmental transport and suggest that shallow groundwater and surface water contamination with tungstate and polytungstate can be expected. Further work will be needed to determine the potential for POMs to solubilize and be transported.

5 Conclusions

Tungsten's chemical speciation and exceptional solubility have important implications regarding its fate in environmental systems, such as the firing ranges in which tungsten munitions were used. The rapid and complete oxidation of tungsten metal is not completely surprising given its instability, but the rate and extent was somewhat unexpected. None of the soils sampled here contained significant tungsten metal, and the other tungsten species in the soil were dispersed throughout the soil matrix.

These results are based on highly contaminated soils but also have implications for the fate of tungsten and other elements in uncontaminated environments. Silica is common in the environment, and its possible complexation with tungstate to form soluble POMs may occur. These POMs would stabilize dissolved tungsten, potentially increasing soluble tungsten concentrations. The toxicity of tungsten could be strongly influenced by the formation of POMs. However, to date, no toxicology studies have been conducted with tungsten POMs. Alternatively, POMs may be sufficiently stable and large that they are soluble but not readily bioavailable, or potentially toxic. Other elements also could form soluble complexes with tungstate. This report's findings suggest that future toxicological studies should consider evaluating POMs as well as tungstate and polytungstate.

This is the first study to identify the presence of POMs in natural soils. Unfortunately, little or no data are available to confirm the presence of the POMs found in this study with other environmental systems. Polytungstates have been observed in a variety of studies (Bednar et al. 2007, 2008), but those studies do not differentiate among polytungstates, nor do they point to the presence of specific POMs. Furthermore, those studies identify polytungstates in solutions in which tungsten should be stable as polytungstates.

Stable POMs of other elements also may be formed in other environments. In fact, the recent identification of aluminum POMs in natural waters appears to significantly alter aluminum solubility and transport in the environment (Furrer et al. 2002). Similar polynuclear complexes are known for molybdate, an important micronutrient in soils, as well as some other elements. Similar complexes could influence tungsten solubility and there

is good reason to believe that the formation of similar POMs could also influence the speciation and fate of other ions in the environment.

The implications of this work can be summarized as follows:

- Tungsten metal was rapidly oxidized from metallic forms to a variety of tungstates, polytungstates, and POMs in soils, leaving little tungsten metal in the soil. The general transformation pathway is as follows:

Metallic Tungsten → Tungsten Oxide → Tungstate → Polytungstate → POM

- Although tungstates, polytungstates, and POMs were identified in soil, it is exceedingly difficult to identify specific polytungstate species or discriminate between mineral phases. Additionally, the similarity in structure between POMs and polytungstates makes their differentiation very difficult.
- The most prevalent forms of oxidized tungsten in surface soils appear to be one or more polytungstates and POMs, which represent the largest fraction of tungsten (and tungstate) in soils and are significantly more abundant than commonly occurring mineral tungstates.
- Tungstate is not predominant in surface soils, which is consistent with its low sorption potential as well as its susceptibility to polymerization. However, what little adsorption that occurs appears to be on iron oxide surfaces, such as ferrihydrite.
- Polyoxometallates have been identified in surface soil soils, the first such observation in natural soils. Polyoxometallates are relatively stable and likely to persist in surface soils and are not likely to migrate significantly.
- In general, POM and polytungstate soil concentrations decline with increasing depth. However, the ratio of tungstate to polytungstate in solution also declined with increasing depth, suggesting higher relative sorption of tungstate versus polytungstate, polymerization of tungstate to polytungstate, or both mechanisms in operation.
- Polytungstates collectively are quite soluble, with soil solutions in desorption experiments containing hundreds of mg L^{-1} tungstate. This solubility in part may be ascribable to weak retention of POMs in soil systems, although more research is needed to fully evaluate their presence and stability. Although polytungstates were not detected in groundwater samples from Camp Edwards, their presence cannot be ruled out.

- Of the many tungsten forms, the potential mobility from highest to lowest is as follows:

  Tungstate → Polytungstate → POM → Tungsten Oxide → Metallic Tungsten

- The weak retention of tungsten, in general, on soils implies that tungsten may be particularly mobile and susceptible to transport to groundwater. Observations of significant tungsten levels in unsaturated soil pore waters under field conditions at Camp Edwards (Clausen and Korte 2009; Clausen et al. 2007, 2010) substantiates tungsten mobility. Furthermore, tungsten has been detected in groundwater at Camp Edwards (Clausen and Korte 2009; Clausen et al. 2010), although the concentrations of tungsten in groundwater are much smaller than concentrations observed in shallow soil pore water. Desorption experiments indicate that soil tungstate, if not properly remediated, can potentially affect shallow groundwater resources. However, the potential mobility is a function of site geochemistry, so tungsten fate-and-transport behavior may be highly variable, necessitating assessment on a case-by-case basis.
- Presence of iron oxides such as ferrihydrite and organic matter may provide a significant control on the mobility of tungsten.

References

Baes, C. F., and R. E. Mesmer. 1986. *The hydrolysis of cations*. 2nd ed. Malabar, FL: Krieger Publishing Company.

Bednar, A. J., R.A. Kirgan, D.R. Johnson, A.L. Russell, C.A. Hayes, and C. J. McGrath. 2009. The use of SEC-ICP-MS and direct infusion ESI-MS for the investigation of polymeric tungsten compounds. *Land contamination reclamation* 17: 1–9.

Bednar, A. J., W. T. Jones, R. E. Boyd, D. B. Ringelberg, and S. L. Larson. 2008. Geochemical parameters influencing tungsten mobility in soils. *Journal of environmental quality* 37: 229–233.

Bednar, A. J., J. E. Mirecki, L. S. Inouye, L. E. Winfield, S. L. Larson, and D. B. Ringelberg. 2007. The determination of tungsten, molybdenum, and phosphorus oxyanions by high performance liquid chromatography inductively coupled plasma mass spectrometry. *Talanta* 72: 1828–1832.

Casey, W. H. 2006. Large aqueous aluminum hydroxide molecules. *Chemical reviews* 106: 1–16.

Chen, Y. G., J. Gong, and L. Y. Qu. 2004. Tungsten-183 nuclear magnetic resonance spectroscopy in the study of polyoxometallates. *Coordination chemistry reviews* 248: 245–260.

Clausen, J., S. Taylor, S. Larson, A. Bednar, M. Ketterer, C. Griggs, D. Lambert, A. Hewitt, C. Ramsey, S. Bigl, R. Bailey, and N. Perron. 2007. *Fate and transport of tungsten at Camp Edwards small arms ranges*. ERDC-CRREL TR–07-05. Hanover, NH: US Army Corps of Engineers, Environmental Research and Development Center, Cold Regions Research and Engineering Laboratory. http://libweb.erdc.usace.army.mil/uhtbin/cgisirsi/20100223144353/SIRSI/0/518/0/ERDC-TR-07-5.pdf/Content/1?new_gateway_db=HYPERION

Clausen, J. L., and N. Korte. 2009. Environmental fate of tungsten from military use. *Science of the total environment* 407: 2887–2893.

Clausen, J. L., A. Bednar, D. Lambert, R. Bailey, M. Kuhlbrush, S. Taylor, and S. Bigl. 2010. *Phase II tungsten fate-and-transport study for Camp Edwards*. ERDC-CRREL TM–10-3. Hanover, NH: US Army Corps of Engineers, Environmental Research and Development Center, Cold Regions Research and Engineering Laboratory.

De Buysser K., I. Van Driessche, P. Vermeir, T. T. Thuy, J. Schaubroeck, and S. Hoste. 2008. EXAFS analysis of blue luminescence in polyoxytungstate citrate gels. *Physica status solidi (b)* 245(11): 2483–2489.

Dermatas, D., W. Braida, C. Christodoulatos, N. Strigul, N. Panikov, M. Los, and S. Larson. 2004. Solubility, sorption, and soil respiration effects of tungsten and tungsten alloys. *Environmental forensics* 5: 5–13.

Dzombak, D. A., and F. M. M. Morel. 1990. *Surface complexation modeling: hydrous ferric oxide*. New York: John Wiley and Sons.

Furrer, G., B. L. Phillips, K. U. Ulrich, R. Pothig, and W. H. Casey. 2002. The origin of aluminum flocs in polluted streams. *Science* 297: 2245–2247.

Gustafsson, J. P. 2003. Modeling molybdate and tungstate adsorption to ferrihydrite. *Chemical geology* 200: 105–115.

Gustafsson, J. P. 2009. *Visual MINTEQ* v. 2.61. Stockholm, Sweden: KTH (Royal Institute of Technology) Department of Land and Water Resources Engineering. http://www.lwr.kth.se/English/OurSoftware/vminteq/

Hartung, M. 1991. Tungsten. In *Metals and their compounds in the environment* (E. Merian Ed.). Weinheim, Germany: VCH, pp. 1269–1272.

Hewitt, A., T. Jenkins, M.E. Walsh, M.R. Walsh, S.R. Bigl, and C.A. Ramsey. 2007. *Protocols for collection of surface soil samples at military training and testing ranges for the characterization of energetic munitions constituents.* ERDC/CRREL TR-07-10. Hanover, NH: Cold Regions Research and Engineering Laboratory, US Army Engineer Research and Development Center. http://libweb.erdc.usace.army.mil/uhtbin/cgisirsi/20100223144516/SIRSI/0/518/0/CRREL-TR-07-10.pdf/Content/1?new_gateway_db=HYPERION

Himeno, S., M. Takamoto, and T. Ueda. 2005. Formation of alpha- and beta-Keggin-type $[PW_{12}O_4](^{3-})$ complexes in aqueous media. *Bulletin of the chemical society of Japan* 78: 1463–1468.

Kelly, S. D., N. Yang, G. E. Mickelson, N. Greenlay, E. Karapetrova, W. Sinkler, and S. R. Bare. 2009. Structural characterization of Ni-W hydrocracking catalysts using in situ EXAFS and HRTEM. *Journal of catalysts* 263: 16–33.

Koopmans, G. F., W. J. Chardon, P. A. I. Ehlert, J. Dolfing, R. A. A. Suurs, O. Oenema, and W. H. van Riemsdijk. 2004. Phosphorus availability for plant uptake in a phosphorus enriched noncalcareous sandy soil. *Journal of environmental quality* 33: 965–975.

Koutsospyros, A., W. Braida, C. Christodoulatos, D. Dermatas, and N. Strigul. 2006. A review of tungsten: From environmental obscurity to scrutiny. *Journal of hazardous materials* 136: 1–19.

Langard, S. 2001. Tungsten. In *Patty's toxicology* (E. Bingham, B. Cohrssen, and C.H. Powell Eds.). New York: John Wiley, pp. 106–128.

Lassner, E., G. Austria, and W.-D. Schubert. 1996. Tungsten, tungsten alloys, and tungsten compounds. In *Ullmann's encyclopedia of industrial chemistry* (B. Elvers and S. Hawkins Eds.). Weinheim, Germany, pp. A27: 229–267.

Manceau, A. 1995. The mechanism of anion adsorption on iron-oxides : Evidence for the bonding of arsenate tetrahedra on free $Fe(O;Oh)(^{6})$ edges. *Geochimica cosmochimica. acta.* 59: 3647–3653.

Manning, B. A., S. E. Fendorf, and S. Goldberg. 1998. Surface structures and stability of arsenic(III) on goethite: Spectroscopic evidence for inner-sphere complexes. *Environmental science and technology* 32: 2383–2388.

Martin, C., P. Malet, G. Solana, and V. Rives. 1998. Structural analysis of silica-supported tungstates. *Journal physical chemistry B* 102: 2759–2768.

Michailovski, A., R. Kiebach, W. Bensch, J. D. Grunwaldt, A. Baiker, S. Komarneni, and G. R. Patzke. 2007. Morphological and kinetic studies on hexagonal tungstates. *Chemical materials* 19: 185–197.

Montanari, B., A. J. Barbosa, S. J. L. Ribeiro, Y. Messaddeq, G. Poirier, and M. S. Li. 2008. Structural study of thin films prepared from tungstate glass matrix by Raman and X-ray absorption spectroscopy. *Applied surface science* 254: 5552–5556.

Morin, G., G. Ona-Nguema, Y. H. Wang, N. Menguy, F. Juillot, O. Proux, F. Guyot, G. Calas, and G. E. Brown. 2008. Extended X-ray absorption fine structure analysis of arsenite and arsenate adsorption on maghemite. *Environmental Science and Technology* 42: 2361–2366.

O'Day, P. A., N. Rivera, R. Root, and S. A. Carroll. 2004. X-ray absorption spectroscopic study of Fe reference compounds for the analysis of natural sediments. *American minerals* 89: 572–585.

Osseo-Asare, K. 1982. Solution chemistry of tungsten leaching systems. *Journal of Metallurgical Transactions* 13B: 555–563.

Pauporte, T., Y. Soldo-Olivier, and R. Faure. 2003. XAS study of amorphous WO3 formation from a peroxo-tungstate solution. *Journal of Physical Chemistry* B 107: 8861–8867.

Schwertmann, U., and R. M. Cornell. 1991. *Iron oxides in the laboratory: Preparation and characterization*. VCH Verlagsgesellschaft: Weinheim.

Strigul, N., A. Koutsospyros, P. Arienti, C. Christodoulatos, D. Dermatas, and W. Braida. 2005. Effects of tungsten on environmental systems. *Chemosphere* 61: 248–258.

Webb, S. M. 2005. SIXPack: A Graphical User Interface for XAS Analysis Using IFEFFIT. *Physica scripta* 115: 1011–1014.

Xu, N., C. Christodoulatos, and W. Braida. 2006. Modeling the competitive effect of phosphate, sulfate, silicate, and tungstate anions on the adsorption of molybdate onto goethite. *Chemosphere* 64: 1325–1333.

Appendix A: Desorption Test Data

Sample ID	Date	Soil	Sample	Mass	Volume	Solid /water	Time	ICP dilu-tion	W_207.9		W_209.4		W_224.8		W_239.7
				g	mL	w/w	hours	factor**	ug/mL	S*	ug/mL	S	ug/mL	S	ug/mL
W012709_1	1/30/09 16:59	soil A	4a	102.1	99.6	1.0	51	56.67	206.8	0.3	209.6	1.0	208.6	0.7	206.3
W012709_2	1/30/09 17:04	soil A	4b	99.55	99.7	1.0	51	56.67	199.0	3.4	200.0	3.1	199.2	3.2	197.0
W012709_3	1/30/09 17:10	soil A	4c	99.77	99.1	1.0	51	56.67	210.1	0.8	210.0	0.9	209.2	0.6	212.5
W012709_4	1/30/09 17:27	soil A	1	209.8	32.0	6.6	51	51.00	865.3	8.8	867.7	8.9	867.1	9.0	868.2
W012709_5	1/30/09 17:33	soil A	2	151.5	31.5	4.8	51	51.00	666.6	3.1	666.9	3.0	664.1	2.4	668.5
W012709_6	1/30/09 17:38	soil A	3	60.87	30.2	2.0	51	51.00	355.7	0.7	354.4	0.8	354.6	0.8	359.4
W012709_7	1/30/09 17:56	soil A	4	30.79	31.6	1.0	51	56.67	206.2	0.8	206.0	0.7	205.7	1.6	208.2
W012709_8	1/30/09 18:01	soil A	5	15.03	31.3	0.5	51	56.67	114.5	0.3	114.4	0.8	114.2	1.0	113.0
W012709_9	1/30/09 18:07	soil A	6	11.94	61.1	0.2	51	56.67	53.9	0.8	54.1	0.9	53.6	1.4	58.4
W012709_10	1/30/09 18:24	soil A	7	12.54	121.6	0.1	51	56.67	33.4	0.3	34.2	0.4	34.9	0.5	35.4
W012709_11	1/30/09 18:30	soil B	1	30.52	30.6	1.0	51	51.00	171.8	1.8	172.4	1.8	174.9	1.9	173.2
W012709_12	1/30/09 18:35	soil C	1	30.73	30.2	1.0	51	56.67	23.7	0.4	23.1	0.3	23.0	0.5	23.3

Sample ID	Date	Soil	Sample	Mass	Volume	Solid /water	Time	ICP dilu-tion	W_207.9		W_209.4		W_224.8		W_239.7
W012709_13	1/30/09 18:53	soil D	1	31.46	30.5	1.0	51	56.67	18.7	0.1	18.4	0.3	18.4	0.3	19.6
W012709_14	1/30/09 18:58	blank	0			n/a	51	56.67	0.0	0.0	0.0	0.0	0.0	0.0	0.0
W012709_1	1/29/09 13:53	soil A	4a			1.0	24	1.00	204.5	3.0	200.4	1.1	206.5	3.1	201.6
W012709_1f	1/29/09 13:58	soil A	4a			1.0	24	1.00	206.5	1.7	200.9	2.4	206.9	1.7	203.3
W012709_2	1/29/09 14:04	soil A	4b			1.0	24	1.00	195.0	2.3	192.0	1.2	195.5	2.7	193.6
W012709_2f	1/29/09 14:10	soil A	4b			1.0	24	1.00	192.0	2.3	191.7	0.6	194.9	2.6	189.9
W012709_3	1/29/09 14:15	soil A	4c			1.0	24	1.00	205.8	4.0	204.0	4.6	208.6	4.2	201.7
W012709_3f	1/29/09 14:21	soil A	4c			1.0	24	1.00	204.4	5.0	200.4	2.8	204.9	5.0	203.1
W012709_14	1/29/09 14:27	blank	0				n/a	24	1.00	0.0	0.0	0.0	0.0	0.0	0.0
W012709_14f	1/29/09 14:32	blank	0				n/a	24	1.00	0.0	0.0	0.0	0.0	0.0	0.0
									MDL 012909	0.006		0.011		0.015	
									MQL 012909	0.019		0.037		0.051	
									MDL 013009	0.016		0.017		0.016	
									MQ 013009	0.052		0.057		0.053	

*uncertainty S reflects measurement uncertainty only and does not include cumulative error from calibration and preparation sources

Sample ID	Date	Soil	Sample	Mass	Volume	Solid /water	Time	ICP dilu-tion	W_207.9		W_209.4		W_224.8		W_239.7
**reported concentrations reflect correction for dilution factor										conc		S			
soil "A" = MMRBMB 03653; MMR range B 95 inc "bullet pocket"									W_NH4 digestA	842	ug/g	17	ug/g		
soil "B" = test MMR B05; MMR T 30-31 trough 0-5cm									W_NH 4digestB	1176	ug/g	12	ug/g		
soil "C" = test MMR B1520; MMR T 30-11 trough 15-20cm									W_NH4 digestC	239	ug/g	6	ug/g		
soil "D" = test MMR B2025; MMR T 30-31 trough 20-25cm									W_NH4 digestD	153	ug/g	6	ug/g		

Media composition																	
				Al2269		**Al3961**		**As1890**		**As1937**		**Ba2335**		**Ba4554**		**Be3130**	
natural water	average			0.023	0.003	0.025	0.002	–0.002	0.003	0.002	0.001	0.021	0.024	0.026	0.031	0.000	0.000
Change in solution composition relative to starting media																	
		W207		**Al2269**		**Al3961**		**As1890**		**As1937**		**Ba2335**		**Ba4554**		**Be3130**	
				Δ		**Δ**		**Δ**		**Δ**		**Δ**		**Δ**		**Δ**	
		ug/mL	**S**	**ug/mL**	**S**	**ug/mL**	**S**	**ug/mL**	**S**	**ug/mL**	**S**	**ug/mL**	**S**	**ug/mL**	**S**	**ug/mL**	**S**
W_012709_N14	2/11/09 14:36	0.0	0.0	–0.004	0.008	–0.012	0.014	0.004	0.008	0.005	0.003	0.000	0.000	0.000	0.000	0.000	0.000
W_012709_N1	2/11/09 14:42	206.8	0.3	0.592	0.056	2.090	0.126	0.187	0.019	–1.034	0.084	0.019	0.003	–0.010	0.000	0.003	0.000
W_012709_N2	2/11/09 14:47	199.0	3.4	0.626	0.033	2.230	0.067	0.199	0.010	–1.109	0.061	0.020	0.002	–0.011	0.000	0.003	0.000
W_012709_N3	2/11/09 15:02	210.1	0.8	0.938	0.054	2.600	0.106	0.206	0.012	–1.168	0.109	0.021	0.003	–0.010	0.000	0.003	0.000
W_012709_N4	2/11/09 15:07	865.3	8.8	0.087	0.025	0.340	0.009	0.030	0.008	–0.179	0.019	–0.004	0.000	–0.010	0.000	0.000	0.000
W_012709_N5	2/11/09 15:13	666.6	3.1	0.094	0.007	0.438	0.025	0.048	0.003	–0.241	0.022	–0.003	0.000	–0.010	0.000	0.001	0.000
W_012709_N6	2/11/09 15:28	355.7	0.7	1.395	0.082	4.113	0.073	0.347	0.026	–1.996	0.127	0.057	0.003	–0.011	0.000	0.006	0.000
W_012709_N7	2/11/09 15:33	206.2	0.8	0.751	0.027	2.368	0.036	0.212	0.010	–1.157	0.054	0.027	0.001	–0.011	0.000	0.003	0.000
W_012709_N8	2/11/09 15:38	114.5	0.3	0.686	0.027	1.589	0.057	0.113	0.005	–0.647	0.042	0.010	0.001	–0.010	0.000	0.002	0.000
W_012709_N9	2/11/09 15:54	53.9	0.8	0.170	0.022	0.478	0.019	0.042	0.002	–0.240	0.022	–0.003	0.000	–0.011	0.000	0.001	0.000
W_012709_N10	2/11/09 15:59	33.4	0.3	0.330	0.017	0.566	0.025	0.034	0.011	–0.185	0.007	–0.005	0.000	–0.010	0.000	0.000	0.000
W_012709_N11	2/11/09 16:04	171.8	1.8	0.203	0.025	0.803	0.036	0.082	0.006	–0.384	0.047	0.002	0.001	–0.011	0.000	0.001	0.000
W_012709_N12	2/11/09 16:20	23.7	0.4	0.307	0.017	0.433	0.003	0.015	0.012	–0.082	0.007	–0.007	0.001	–0.010	0.000	0.000	0.000
W_012709_N13	2/11/09 16:25	18.7	0.1	0.325	0.010	0.432	0.004	0.022	0.004	–0.067	0.004	–0.007	0.000	–0.010	0.000	0.000	0.000

Media composition															
		Ca1840		**Ca3179**		**Cd2144**		**Cd2288**		**Ce4133**		**Ce4460**		**Co2286**	
natural water	average	3.416	0.051	3.342	0.047	0.000	0.000	0.000	0.000	0.225	0.095	0.207	0.125	0.000	0.000
Change in solution composition relative to starting media															
		Ca1840		**Ca3179**		**Cd2144**		**Cd2288**		**Ce4133**		**Ce4460**		**Co2286**	
		Δ		**Δ**		**Δ**		**Δ**		**Δ**		**Δ**		**Δ**	
		ug/mL	**S**	**ug/mL**	**S**	**ug/mL**	**S**	**ug/mL**	**S**	**ug/mL**	**S**	**ug/mL**	**S**	**ug/mL**	**S**
W_012709_N14	2/11/09 14:36	0.005	0.034	–0.072	0.006	0.002	0.000	0.000	0.000	–0.197	0.373	0.158	–0.261	0.001	0.001
W_012709_N1	2/11/09 14:42	95.714	0.265	90.410	0.239	–0.260	0.021	0.017	0.001	–0.335	0.283	5.870	–0.199	–0.024	0.003
W_012709_N2	2/11/09 14:47	93.591	1.392	88.641	0.237	–0.274	0.013	0.018	0.001	–0.383	0.266	6.116	–0.058	–0.025	0.001
W_012709_N3	2/11/09 15:02	96.254	0.133	90.007	0.191	–0.281	0.021	0.019	0.002	–0.373	0.245	5.749	–0.380	–0.025	0.003
W_012709_N4	2/11/09 15:07	6.111	0.048	5.970	0.030	–0.043	0.003	0.003	0.000	0.005	0.176	0.328	–0.289	–0.004	0.001
W_012709_N5	2/11/09 15:13	8.431	0.149	7.826	0.023	–0.057	0.005	0.004	0.000	–0.312	0.224	0.587	–0.246	–0.005	0.001
W_012709_N6	2/11/09 15:28	118.321	1.248	117.441	0.372	–0.397	0.004	0.033	0.002	–0.387	0.054	7.834	–0.350	–0.054	0.003
W_012709_N7	2/11/09 15:33	92.246	0.515	91.102	0.578	–0.304	0.010	0.019	0.001	–0.120	0.330	5.774	–0.102	–0.030	0.002
W_012709_N8	2/11/09 15:38	71.162	0.285	68.316	0.363	–0.167	0.009	0.011	0.000	–0.350	0.085	5.077	–0.443	–0.016	0.001
W_012709_N9	2/11/09 15:54	50.739	0.123	48.183	0.565	–0.062	0.006	0.004	0.001	–0.120	0.614	3.184	–0.318	–0.005	0.000
W_012709_N10	2/11/09 15:59	38.029	0.136	35.388	0.289	–0.045	0.002	0.003	0.000	–0.177	0.464	2.590	–0.241	–0.004	0.000
W_012709_N11	2/11/09 16:04	89.763	0.576	89.049	0.188	–0.100	0.010	0.006	0.001	–0.215	0.261	6.207	–0.194	–0.009	0.001
W_012709_N12	2/11/09 16:20	56.584	0.084	53.250	0.408	–0.024	0.001	0.002	0.000	–0.292	0.487	3.544	–0.118	–0.002	0.000
W_012709_N13	2/11/09 16:25	65.565	0.185	62.253	0.614	–0.018	0.001	0.002	0.001	–0.378	0.315	4.375	–0.418	–0.001	0.000

Media composition															
		Co2307		**Cr2677**		**Cr2835**		**Cu2247**		**Cu3247**		**Fe2382**		**Fe2599**	
natural water	average	0.000	0.002	–0.001	0.003	0.000	0.001	0.001	0.001	0.004	0.002	0.054	0.005	0.056	0.001
Change in solution composition relative to starting media															
		Co2307		**Cr2677**		**Cr2835**		**Cu2247**		**Cu3247**		**Fe2382**		**Fe2599**	
		Δ		**Δ**		**Δ**		**Δ**		**Δ**		**Δ**		**Δ**	
		ug/mL	**S**	**ug/mL**	**S**	**ug/mL**	**S**	**ug/mL**	**S**	**ug/mL**	**S**	**ug/mL**	**S**	**ug/mL**	**S**
W_012709_N14	2/11/09 14:36	0.002	0.003	0.000	0.002	0.000	0.001	0.009	0.001	–0.001	0.000	0.001	0.004	0.001	0.004
W_012709_N1	2/11/09 14:42	0.240	0.020	0.181	0.009	0.059	0.004	–0.394	0.066	0.421	0.001	0.067	0.015	0.052	0.012
W_012709_N2	2/11/09 14:47	0.253	0.014	0.191	0.004	0.060	0.003	–0.452	0.048	0.409	0.001	0.033	0.012	0.015	0.005
W_012709_N3	2/11/09 15:02	0.264	0.023	0.210	0.007	0.067	0.003	–0.445	0.087	0.447	0.005	0.199	0.011	0.170	0.008
W_012709_N4	2/11/09 15:07	0.041	0.002	0.028	0.001	0.008	0.001	–0.101	0.012	0.037	0.002	–0.064	0.006	–0.057	0.000
W_012709_N5	2/11/09 15:13	0.054	0.003	0.037	0.002	0.012	0.001	–0.134	0.013	0.043	0.001	–0.072	0.004	–0.070	0.010
W_012709_N6	2/11/09 15:28	0.509	0.035	0.343	0.014	0.127	0.004	–1.305	0.103	0.542	0.002	–0.057	0.023	–0.044	0.022
W_012709_N7	2/11/09 15:33	0.285	0.013	0.204	0.005	0.067	0.002	–0.618	0.038	0.407	0.006	0.043	0.018	0.044	0.004
W_012709_N8	2/11/09 15:38	0.156	0.006	0.110	0.003	0.036	0.001	–0.227	0.029	0.313	0.006	0.238	0.006	0.210	0.005
W_012709_N9	2/11/09 15:54	0.058	0.004	0.043	0.003	0.012	0.003	–0.055	0.016	0.140	0.002	0.063	0.009	0.058	0.003
W_012709_N10	2/11/09 15:59	0.043	0.006	0.032	0.002	0.009	0.001	–0.016	0.004	0.117	0.003	0.216	0.011	0.193	0.001
W_012709_N11	2/11/09 16:04	0.095	0.010	0.065	0.001	0.021	0.001	0.018	0.032	0.361	0.003	–0.068	0.012	–0.068	0.007
W_012709_N12	2/11/09 16:20	0.025	0.004	0.018	0.002	0.005	0.003	0.065	0.003	0.138	0.003	0.100	0.008	0.087	0.002
W_012709_N13	2/11/09 16:25	0.020	0.002	0.015	0.004	0.003	0.003	0.039	0.003	0.099	0.003	0.153	0.004	0.130	0.005

Media composition															
		K_7664		**Li6707**		**Mg2790**		**Mg2852**		**Mn2576**		**Mn2605**		**Mo2038**	
natural water	average	0.832	0.016	0.001	0.001	0.967	0.013	0.913	0.012	0.001	0.000	0.001	0.001	0.000	0.002
Change in solution composition relative to starting media															
		K_7664		**Li6707**		**Mg2790**		**Mg2852**		**Mn2576**		**Mn2605**		**Mo2038**	
		Δ		**Δ**		**Δ**		**Δ**		**Δ**		**Δ**		**Δ**	
		ug/mL	**S**	**ug/mL**	**S**	**ug/mL**	**S**	**ug/mL**	**S**	**ug/mL**	**S**	**ug/mL**	**S**	**ug/mL**	**S**
W_012709_N14	2/11/09 14:36	–0.024	0.032	0.000	0.000	–0.002	0.032	0.010	0.002	0.000	0.000	0.001	0.001	–0.002	0.002
W_012709_N1	2/11/09 14:42	1.348	0.012	0.005	0.001	2.819	0.032	3.193	0.017	0.075	0.001	0.005	0.003	–0.045	0.007
W_012709_N2	2/11/09 14:47	1.337	0.010	0.004	0.001	2.657	0.009	3.124	0.011	0.074	0.000	0.000	0.002	–0.044	0.005
W_012709_N3	2/11/09 15:02	1.379	0.001	0.005	0.001	2.716	0.067	3.227	0.019	0.081	0.001	0.002	0.002	–0.047	0.005
W_012709_N4	2/11/09 15:07	–0.605	0.017	–0.001	0.001	–0.571	0.029	–0.429	0.001	0.007	0.000	–0.004	0.002	–0.005	0.001
W_012709_N5	2/11/09 15:13	–0.610	0.027	0.001	0.001	–0.526	0.017	–0.343	0.004	0.009	0.001	–0.006	0.001	–0.010	0.003
W_012709_N6	2/11/09 15:28	1.638	0.042	0.006	0.002	4.427	0.059	4.507	0.054	0.123	0.001	–0.021	0.001	–0.103	0.009
W_012709_N7	2/11/09 15:33	1.236	0.018	0.004	0.001	2.760	0.020	2.996	0.013	0.080	0.000	–0.002	0.001	–0.055	0.004
W_012709_N8	2/11/09 15:38	1.006	0.023	0.002	0.001	2.011	0.032	2.201	0.019	0.052	0.001	0.009	0.001	–0.029	0.002
W_012709_N9	2/11/09 15:54	0.647	0.020	0.001	0.001	0.890	0.008	0.974	0.005	0.027	0.001	0.010	0.001	–0.011	0.002
W_012709_N10	2/11/09 15:59	0.419	0.025	0.002	0.001	0.481	0.021	0.547	0.003	0.019	0.000	0.009	0.000	–0.009	0.002
W_012709_N11	2/11/09 16:04	1.772	0.046	0.002	0.000	2.916	0.028	2.900	0.006	0.058	0.000	0.032	0.002	–0.010	0.002
W_012709_N12	2/11/09 16:20	1.503	0.013	0.002	0.000	1.710	0.008	1.644	0.006	0.039	0.000	0.034	0.001	–0.002	0.001
W_012709_N13	2/11/09 16:25	1.179	0.016	0.001	0.001	1.976	0.015	1.949	0.017	0.048	0.001	0.043	0.002	0.000	0.001

Media composition															
		Mo2045		**Na5895**		**Na8183**		**Ni2216**		**Ni2316**		**P_1774**		**P_1782**	
natural water	average	–0.001	0.000	24.339	0.359	25.135	0.387	–0.019	0.000	0.001	0.000	0.007	0.004	0.003	0.006
Change in solution composition relative to starting media															
		Mo2045		**Na5895**		**Na8183**		**Ni2216**		**Ni2316**		**P_1774**		**P_1782**	
		Δ		**Δ**		**Δ**		**Δ**		**Δ**		**Δ**		**Δ**	
		ug/mL	**S**	**ug/mL**	**S**	**ug/mL**	**S**	**ug/mL**	**S**	**ug/mL**	**S**	**ug/mL**	**S**	**ug/mL**	**S**
W_012709_N14	2/11/09 14:36	0.000	0.002	0.332	0.065	0.456	0.254	–0.010	0.002	0.000	0.002	–0.025	0.003	–0.008	0.014
W_012709_N1	2/11/09 14:42	–0.019	0.003	–3.383	0.054	–3.317	0.117	0.795	0.083	–0.011	0.001	75.732	0.431	76.602	0.245
W_012709_N2	2/11/09 14:47	–0.020	0.003	–3.406	0.103	–3.358	0.073	0.845	0.057	–0.010	0.001	76.358	0.711	77.716	0.812
W_012709_N3	2/11/09 15:02	–0.021	0.004	–3.414	0.089	–3.441	0.052	0.889	0.098	–0.011	0.002	77.795	0.285	79.457	0.214
W_012709_N4	2/11/09 15:07	–0.003	0.001	–21.516	0.012	–22.223	0.138	0.159	0.014	–0.002	0.001	5.250	0.077	5.140	0.021
W_012709_N5	2/11/09 15:13	–0.006	0.002	–21.576	0.007	–22.067	0.121	0.211	0.017	–0.004	0.001	5.742	0.108	5.656	0.107
W_012709_N6	2/11/09 15:28	–0.037	0.007	–4.378	0.236	–4.753	0.262	1.738	0.152	–0.024	0.002	89.059	1.045	85.646	1.485
W_012709_N7	2/11/09 15:33	–0.022	0.004	–3.015	0.101	–3.330	0.094	0.972	0.051	–0.015	0.002	76.453	0.461	74.614	0.276
W_012709_N8	2/11/09 15:38	–0.014	0.001	–2.006	0.151	–1.988	0.215	0.512	0.033	–0.007	0.001	62.516	0.053	62.170	0.277
W_012709_N9	2/11/09 15:54	–0.003	0.001	–0.459	0.120	–0.334	0.100	0.181	0.026	–0.002	0.001	44.761	0.124	44.784	0.328
W_012709_N10	2/11/09 15:59	–0.002	0.000	–0.131	0.024	0.140	0.269	0.143	0.006	–0.002	0.001	32.891	0.056	33.622	0.047
W_012709_N11	2/11/09 16:04	0.000	0.002	–9.677	0.020	–10.040	0.335	0.182	0.038	–0.002	0.001	27.358	0.352	26.974	0.203
W_012709_N12	2/11/09 16:20	0.003	0.001	–4.444	0.106	–4.684	0.154	–0.014	0.007	0.001	0.000	31.934	0.247	32.413	0.247
W_012709_N13	2/11/09 16:25	0.001	0.002	–4.372	0.137	–4.483	0.076	–0.037	0.003	0.003	0.001	45.182	0.134	46.081	0.266

Media composition															
		Pb1682		**Pb2203**		**S_1807**		**S_1820**		**Si2124**		**Si2516**		**Sr3464**	
natural water	average	10.887	27.686	0.000	0.002	2.267	0.037	2.262	0.030	0.000	0.000	0.000	0.000	0.039	0.001
Change in solution composition relative to starting media															
		Pb1682		**Pb2203**		**S_1807**		**S_1820**		**Si2124**		**Si2516**		**Sr3464**	
		Δ		**Δ**		**Δ**		**Δ**		**Δ**		**Δ**		**Δ**	
		ug/mL	**S**	**ug/mL**	**S**	**ug/mL**	**S**	**ug/mL**	**S**	**ug/mL**	**S**	**ug/mL**	**S**	**ug/mL**	**S**
W_012709_N14	2/11/09 14:36	6.156	4.627	0.018	0.005	0.035	0.014	0.041	0.014	0.000	0.000	0.000	0.000	0.001	0.003
W_012709_N1	2/11/09 14:42	0.207	5.977	–2.013	0.161	8.164	0.026	4.872	0.176	0.000	0.000	0.000	0.000	0.050	0.001
W_012709_N2	2/11/09 14:47	–2.269	6.973	–2.136	0.103	7.995	0.155	4.531	0.211	0.000	0.000	0.000	0.000	0.051	0.004
W_012709_N3	2/11/09 15:02	–8.152	3.712	–2.199	0.211	8.215	0.017	4.589	0.204	0.000	0.000	0.000	0.000	0.050	0.004
W_012709_N4	2/11/09 15:07	1.535	5.809	–0.325	0.030	–0.667	0.012	–1.131	0.020	0.000	0.000	0.000	0.000	–0.028	0.003
W_012709_N5	2/11/09 15:13	–1.565	13.289	–0.440	0.037	–0.113	0.011	–0.741	0.032	0.000	0.000	0.000	0.000	–0.021	0.001
W_012709_N6	2/11/09 15:28	–7.200	7.343	–4.453	0.335	13.118	0.167	7.715	0.182	0.000	0.000	0.000	0.000	0.255	0.004
W_012709_N7	2/11/09 15:33	2.308	12.188	–2.378	0.090	7.825	0.047	4.421	0.150	0.000	0.000	0.000	0.000	0.047	0.002
W_012709_N8	2/11/09 15:38	2.231	5.600	–1.231	0.063	5.029	0.008	2.903	0.070	0.000	0.000	0.000	0.000	0.153	0.004
W_012709_N9	2/11/09 15:54	–1.786	6.468	–0.459	0.050	2.891	0.016	1.866	0.067	0.000	0.000	0.000	0.000	–0.004	0.003
W_012709_N10	2/11/09 15:59	0.201	10.042	–0.317	0.009	2.067	0.016	1.241	0.032	0.000	0.000	0.000	0.000	–0.003	0.001
W_012709_N11	2/11/09 16:04	4.218	4.543	–0.753	0.069	11.797	0.089	10.201	0.052	0.000	0.000	0.000	0.000	–0.009	0.005
W_012709_N12	2/11/09 16:20	1.186	5.397	–0.130	0.019	4.125	0.023	3.356	0.011	0.000	0.000	0.000	0.000	–0.021	0.001
W_012709_N13	2/11/09 16:25	–3.310	1.885	–0.078	0.005	5.417	0.039	4.617	0.009	0.000	0.000	0.000	0.000	–0.022	0.001

Media composition											
		Sr4077		**V_2924**		**V_3102**		**Zn2062**		**Zn2138**	
natural water	average	0.039	0.000	–0.001	0.001	–0.001	0.002	0.007	0.001	0.005	0.000
Change in solution composition relative to starting media											
		Sr4077		**V_2924**		**V_3102**		**Zn2062**		**Zn2138**	
		Δ		**Δ**		**Δ**		**Δ**		**Δ**	
		ug/mL	**S**	**ug/mL**	**S**	**ug/mL**	**S**	**ug/mL**	**S**	**ug/mL**	**S**
W_012709_N14	2/11/09 14:36	0.000	0.000	–0.002	0.002	0.000	0.001	0.001	0.001	0.000	0.000
W_012709_N1	2/11/09 14:42	0.016	0.000	0.082	0.001	0.099	0.001	0.089	0.006	0.002	0.001
W_012709_N2	2/11/09 14:47	0.015	0.000	0.086	0.002	0.096	0.003	0.093	0.005	0.001	0.001
W_012709_N3	2/11/09 15:02	0.013	0.000	0.090	0.004	0.107	0.002	0.103	0.008	0.005	0.000
W_012709_N4	2/11/09 15:07	–0.030	0.000	0.010	0.002	0.012	0.001	0.012	0.000	–0.004	0.000
W_012709_N5	2/11/09 15:13	–0.030	0.000	0.012	0.002	0.011	0.002	0.018	0.003	–0.003	0.000
W_012709_N6	2/11/09 15:28	0.183	0.002	0.139	0.002	0.160	0.002	0.163	0.013	0.001	0.001
W_012709_N7	2/11/09 15:33	0.010	0.000	0.092	0.005	0.112	0.003	0.095	0.004	0.002	0.000
W_012709_N8	2/11/09 15:38	0.130	0.001	0.062	0.001	0.072	0.001	0.057	0.002	0.004	0.000
W_012709_N9	2/11/09 15:54	–0.010	0.000	0.029	0.001	0.037	0.002	0.021	0.002	–0.001	0.000
W_012709_N10	2/11/09 15:59	–0.012	0.000	0.022	0.001	0.025	0.001	0.020	0.000	0.001	0.000
W_012709_N11	2/11/09 16:04	–0.019	0.000	0.041	0.001	0.050	0.002	0.028	0.002	–0.003	0.000
W_012709_N12	2/11/09 16:20	–0.023	0.000	0.032	0.004	0.043	0.002	0.010	0.000	–0.001	0.000
W_012709_N13	2/11/09 16:25	–0.024	0.000	0.028	0.002	0.036	0.003	0.006	0.001	–0.003	0.000

REPORT DOCUMENTATION PAGE

Form Approved
OMB No. 0704-0188

1. REPORT DATE *(DD-MM-YYYY)*	2. REPORT TYPE	3. DATES COVERED *(From - To)*
January 2011	Final	

4. TITLE AND SUBTITLE

Tungsten Speciation in Firing Range Soils

5a. CONTRACT NUMBER

5b. GRANT NUMBER

5c. PROGRAM ELEMENT NUMBER

6. AUTHOR(S)

Jay L. Clausen, Benjamin C. Bostick, Anthony Bednar, Jing Sun, and Joshua D. Landis

5d. PROJECT NUMBER

5e. TASK NUMBER

5f. WORK UNIT NUMBER

7. PERFORMING ORGANIZATION NAME(S) AND ADDRESS(ES)

U.S. Army Engineer Research and Development Center
72 Lyme Road
Hanover, NH 03755

8. PERFORMING ORGANIZATION REPORT NUMBER

ERDC TR-11-1

9. SPONSORING / MONITORING AGENCY NAME(S) AND ADDRESS(ES)

U.S. Army Environmental Command, 5179 Hoadley Road, Aberdeen Proving Ground, MD

10. SPONSOR/MONITOR'S ACRONYM(S)

11. SPONSOR/MONITOR'S REPORT NUMBER(S)

12. DISTRIBUTION / AVAILABILITY STATEMENT

Approved for public release; distribution is unlimited.

13. SUPPLEMENTARY NOTES

14. ABSTRACT

Synchrotron-based X-ray absorption spectroscopy (XAS) of select surface soil samples obtained from Camp Edwards, Massachusetts, small arms ranges indicate that little tungsten metal remains in the soil and that is not stable in the natural environment. X-ray absorption near edge structure (XANES) studies indicate rapid oxidation of tungsten metal to form tungsten oxides W(VI), polytungstates, tungstates, and polyoxometallates (POM) in any number of forms. Owing to structural similarities, it is difficult to identify specific species or discriminate between mineral species, although polytungstates and POMs predominate as compared to tungstates in soil. Additionally, this is the first study to identify the presence of tungsten POMs in soil. XANES spectra indicated that, as depth increased, the fraction of soil sorbed tungstate increased and both polytungstate and POM decreased, suggesting POM and polytungstates are more stable in surface soils and likely to persist, whereas tungstate is unstable. Tetrahedral tungstate is unstable in neutral and acidic pH solutions such as are present in Camp Edwards surface soils, resulting in its conversion to a variety of polytungstates. Adsorption of tungstate, although weak, appears to occur on iron oxide surfaces such as ferrihydrite. XAS studies also revealed prevalence of adsorbed polytungstates rather than discrete mineral phases. (Cont'd).

15. SUBJECT TERMS

Environmental cleanup
Polyoxometallates
Polytungstate
Speciation
Tungstate
Tungsten
UXO

16. SECURITY CLASSIFICATION OF:			17. LIMITATION OF ABSTRACT	18. NUMBER OF PAGES	19a. NAME OF RESPONSIBLE PERSON
a. REPORT	b. ABSTRACT	c. THIS PAGE			19b. TELEPHONE NUMBER *(include area code)*
Unclassified	Unclassified	Unclassified	Unclassified	83	

ABSTRACT (cont'd)

Soil pore waters in equilibrium with contaminated soils during laboratory experiments yielded tungsten concentrations in excess of 5000 mg L^{-1}, considerably in excess of predicted solubility limits of common tungsten minerals. These findings are consistent with field observations whereby tension lysimeters installed in the shallow vadose zone to monitor the soil pore water at the Bravo Range at Camp Edwards had tungsten concentrations as high as 400 mg L^{-1}. The high solubility and limited adsorption of tungsten in these soils is attributed to the formation of POMs such as $W_{12}SiO_{40}^{4-}$, an α-Keggin cluster, in soil solutions in addition to other polytungstates. Polytungstates are quite soluble and can yield water concentrations of several hundred mg L^{-1}. Although, not detected in groundwater, possibly because of analytical limitations, the presence of polytungstates in the vadose zone pore water at Camp Edwards suggests their presence cannot be completely ruled out. In contrast, the presence of tungstates in groundwater has been confirmed at Camp Edwards. The weak retention of tungsten, in general to soils and observation of tungsten in soil pore water and groundwater at Camp Edwards attests to tungsten's potential mobility and transport in groundwater. The slow rates of conversion between POMs, polytungstates, and tungstates are likely to affect their solubility and transport considerably. Additionally, the presence of iron oxides such as ferrihydrite and organic matter may limit tungsten mobility. In general, tungsten mobility from highest to lowest proceeds from Tungstate → Polytungstate → POM → Tungsten Oxide → Metallic Tungsten.